Circadian control of a sex-specific behaviour in Drosophila

Sabrina Riva[1], M. Fernanda Ceriani[2], Sebastián Risau-Gusman[1]* and D. Lorena Franco[1]*

1- Medical Physics Department, Bariloche Atomic Center, Comisión Nacional de Energía Atómica (CNEA) and Consejo Nacional de Investigaciones Científicas y Técnicas (CONICET), San Carlos de Bariloche, Argentina

2- Laboratorio de Genética del Comportamiento. Fundación Instituto Leloir - IIBBA - CONICET, Buenos Aires, C1405BWE, Argentina

* Shared corresponding authors.

E-mail: lorena.franco@cab.cnea.gov.ar; srisau@cab.cnea.gov.ar

ABSTRACT

An endogenous circadian clock controls many of the behavioral traits of *Drosophila melanogaster*. This ¨clock¨ relies on the activity of interconnected clusters of neurons that harbor the clock machinery. The hierarchy among clusters involved in the control of rest-activity cycles has been extensively studied. Sexually dimorphic behaviors, on the other hand, have received less attention. Even though egg-laying, a female characteristic behavior, has been shown to be rhythmic, it remains largely unexplored possibly due to metholodological constraints. The current study provides the first steps towards determining the neural substrates underlying the circadian control of egg-laying. We show that, whereas the lateral ventral neurons (LNvs) and the dorsal neurons (DNs) are dispensable, the lateral dorsal neurons (LNds) are necessary for rhythmic egg-laying. Systematically probing the *Drosophila* connectome for contacts between circadian clusters and oviposition-related neurons, we found no evidence of direct connections between LNvs or DNs and neurons recruited during oviposition. Conversely, we did find bidirectional connections between Cryptochrome (Cry)

26 expressing LNd (Cry+ LNds) and oviposition related neurons. Taken together, these results reveal that
27 Cry+ LNd neurons have a leading role in the control of the egg-laying rhythm in *Drosophila* females.
28

29 **INTRODUCTION**

30 Most organisms are capable of coordinating their physiology and behavior with the 24 hours of
31 day/night cycling generated by the Earth´s rotation. These biological rhythms are driven by
32 molecular clocks that are conserved across animals (Allada et al., 2001). In *Drosophila melanogaster*
33 the core clock components comprise a transcription/translation feedback loop with four core
34 proteins: CLOCK (CLK) CYCLE (CYC), PERIOD (PER), and TIMELESS (TIM) (Hardin, 2005; Tataroglu and
35 Emery, 2015). In brief, CLK and CYC activate transcription of *period* and *timeless* genes, which, once
36 translated into PER and TIM proteins, dimerize and translocate into the nucleus where they bind to
37 CLK and CYC, thereby inhibiting their own transcription. This molecular feedback loop has a period
38 of approximately 24 hours. In the *Drosophila* brain this molecular circadian clock is expressed in ~
39 242 neurons, which are organized in different clusters based in gene expression, anatomy and
40 localization (Helfrich-Förster, 2005a; Reinhard et al., 2024; Yoshii et al., 2012). These clusters are:
41 ventrolateral neurons (LNv; encompassing the small and large LNv groups), dorsolateral neurons
42 (LNd), lateral posterior (LPN), and dorsal neurons [DN; separated in DN1, 2, and 3 and further
43 subdivided into anterior (DN1a) and posterior (DN1p) DN1]. Rhythmic locomotor behavior depends
44 primarily on the activity of the sLNvs, LNds, and DN1s, but all clusters contribute to different extents
45 (Helfrich-Förster, 2005b). Within the lateral neuron group, the sLNv are important because they
46 drive locomotor rhythmicity under free-running (DD) conditions (Grima et al., 2004; Stoleru et al.,
47 2004), through the release of Pigment Dispersing Factor (PDF), a neuropeptide relevant for
48 communication between clock neurons (Renn et al., 1999; Yoshii et al., 2009).
49 Egg-laying is one of the most important female behaviors since it has a profound impact on the
50 fitness of a species. Egg laying is largely governed by successful mating, but is also influenced by

51 circadian and seasonal rhythms and by environmental factors such as temperature and food
52 availability, among others (Cury et al., 2019). The circadian rhythm of oviposition is one of the less
53 studied rhythms in *Drosophila*, possibly due to the challenges involved in monitoring and recording
54 this behavior. The periodic deposition of eggs involves a series of events ranging from the production
55 of oocytes to the choice of the most appropriate substrate for the eggs (Allemand, 1976; Yang et
56 al., 2008). The circadian nature of this behavior was revealed by its persistence under DD with a
57 period around 24 h and a peak near night onset (McCabe and Birley, 1998a; Sheeba et al., 2001a).
58 Egg-laying rhythmicity is temperature and nutrition compensated. (Howlader et al., 2006a).
59 Moreover, oviposition is rhythmic in virgin females as well as in mated ones suggesting that this
60 rhythm is not regulated by the act of mating and, instead, is endogenously driven (Menon et al.,
61 2014a).
62 Although oviposition exhibits a circadian component, the molecular and neural substrates that
63 govern this rhythm have only been partially described (Howlader et al., 2006b). Here, using an
64 automated egg collection device developed in our lab, we examined the contribution of the
65 molecular clock in specific neuronal clusters. By downregulating *per* in subsets of circadian neurons,
66 we determined that even though impairing the molecular clock in the entire clock network reduced
67 the power of the circadian rhythm of oviposition, restricting the disruption to DN1ps or LNvs did not
68 (confirming results obtained by Howlader et al., 2006 for the sLNv (Howlader et al., 2006b)).
69 Interestingly, egg-laying rhythms disappeared upon targeting a subset of LNd clocks (Cry+ LNd)
70 through RNAi-mediated *per* downregulation, a condition where rhythmicity of locomotor activity
71 patterns remained unaltered, suggesting a leading and very specific role of LNd clocks/neurons in
72 the control of oviposition. Finally, the assessment of the synaptic connectivity between clock and
73 oviposition controlling neurons using the Janelia hemibrain dataset revealed direct synaptic
74 connections between this subset of LNds and oviposition neurons, which is consistent with the
75 essential role of LNds neurons in the control of this behavior.

RESULTS

Egg-laying is rhythmic when registered with a semiautomated egg collection device

Oviposition in *Drosophila* is one of the less studied behaviors regulated by the circadian clock. This is probably due to the difficulties involved in monitoring and recording it, and the current lack of standard devices to accomplish this. Egg collection and counting is usually done manually, making the experiments particularly demanding and labor-intensive. In this approach, eggs are typically collected every 4 hours (sometimes also every 2 hours), which usually implies transferring the fly to a new vial or extracting the food with the eggs and replacing it with fresh food in the same vial (Menon et al., 2014b). **¡Error! Marcador no definido.**Either way this implies disturbing the fly several times a day which could alter the normal rhythm of oviposition, and demands the intervention of an experimenter every 4 hours during several days. In order to avoid this, we developed a semiautomated egg collection device where 21 flies are individually housed, and each enclosure is slowly shifted every 4 hours from one food patch to a new food patch. Once per day all food patches are collected and eggs are manually counted (see **Material and Methods; Figure supplement 1 and supplementary video** for more details).

The egg records of fruit flies display several distinct features that complicate the assessment of rhythmicity. The recorded variable is discrete and typically takes only a few values, depending on the sampling frequency. The more often it is sampled, the fewer number of values the variable takes. Thus, it is only possible to sample it a few times per cycle (usually less than ten). For noisy signals, this feature makes the assessment of rhythmicity much more complicated, compared with signals that have similar noise, but are sampled more frequently (as is the case for activity records). The particularities of egg-laying in *Drosophila* add further complications. First, the number of eggs laid shows a clear decreasing trend over time. Second, this behavior appears to be particularly "noisy",

in the sense that the decision to lay an egg depends not only on the time of the day, but also on many other stimuli (Cury et al., 2019). As a consequence, any method that tries to assess the presence of a rhythm must be able to subtract, at least partially, the effects of trend and noise.

In order to achieve this, we have considered the register of the eggs laid by a "rhythmic" female as a periodic signal corrupted by random noise (whereas for arrhythmic females we assume the record is completely random). It is well known that light is a powerful zeitgeber for activity, synchronizing all the flies in a population to the light-dark (LD) cycle, and that even after lights off, activity remains synchronized between flies for quite a long time. Since this is caused by the synchronization of cellular clocks, we assume that a similar effect occurs for oviposition.. Thus, under LD conditions, or in the first days of DD, it can be assumed that the periodic signal is the same for all flies, whereas the noisy component is different for each individual. In this case it is well known (see e.g. (van Drongelen, 2007)) that averaging of several "replicates" (individual flies, in our case) leads to an improvement of the signal-to-noise ratio allowing the emergence of the underlying rhythm. As this approach seems to be better suited for detecting noisy rhythms, in the rest of the paper the assessment of rhythmicity will be based in the record of eggs laid during a given period of time averaged over all females of each genotype. **Figure 1** shows that, when eggs are collected with our device in LD, *Canton-S* females have a peak of egg deposition at the end of the day, as previously described in the literature (Bailly et al., 2023; Howlader et al., 2006a; Sheeba et al., 2001b) (**Figure 1A**). **Figure 1E** shows that only about 70% of individuals are rhythmic (with a period close to 24 h**Figure 1F**) although the average egg-laying profile is robust with a period around 24 h (**Figure 1B**). Under DD conditions, the percentages of rhythmic individuals is the same as in LD (**Figure 1E**) and the average profile also shows a robust rhythm with a period of 24 h (**Figure 1D**). It is well known that in locomotor activity experiments more than 90% of the flies are rhythmic in DD, and virtually all flies are rhythmic in LD (see e.g. Shindey et al. 2016, and Deppisch et al. 2022 (Deppisch et al., 2022; Shindey et al., 2017)). This shows that, at the individual level, egg-laying is much less robust

126 than locomotor activity, compounding the difficulty of observing the influence of the circadian clock
127 on this behavior.
128 In order to check that our egg collection device does not in any way entrain egg laying in flies, we
129 tested it with perS mutants (Konopka and Benzer, 1971). These flies are known to display a short
130 period of locomotor activity, both in males (Konopka and Benzer, 1971) and in females (McCabe
131 and Birley, 1998b). Additionally, it has been shown that oviposition in perS flies is rhythmic, with a
132 period of 20.6+/- 0.9h (McCabe and Birley, 1998b). Our results for this mutant are in agreement
133 with this (**Figure 1J** shows a period of the average at 18.8+/- 1.1 h), thus confirming that flies are not
134 entrained by our egg collection device. It is important to notice that in the *yellow white* (*YW*) control
135 strain, the individual rhythmicity was rather low (around 50% **Figure 1K**), but the average is strongly
136 rhythmic (**Figure 1H**) thus confirming the need for an analysis method that can take into account the
137 low signal-to-noise-ratio of this behavior.
138

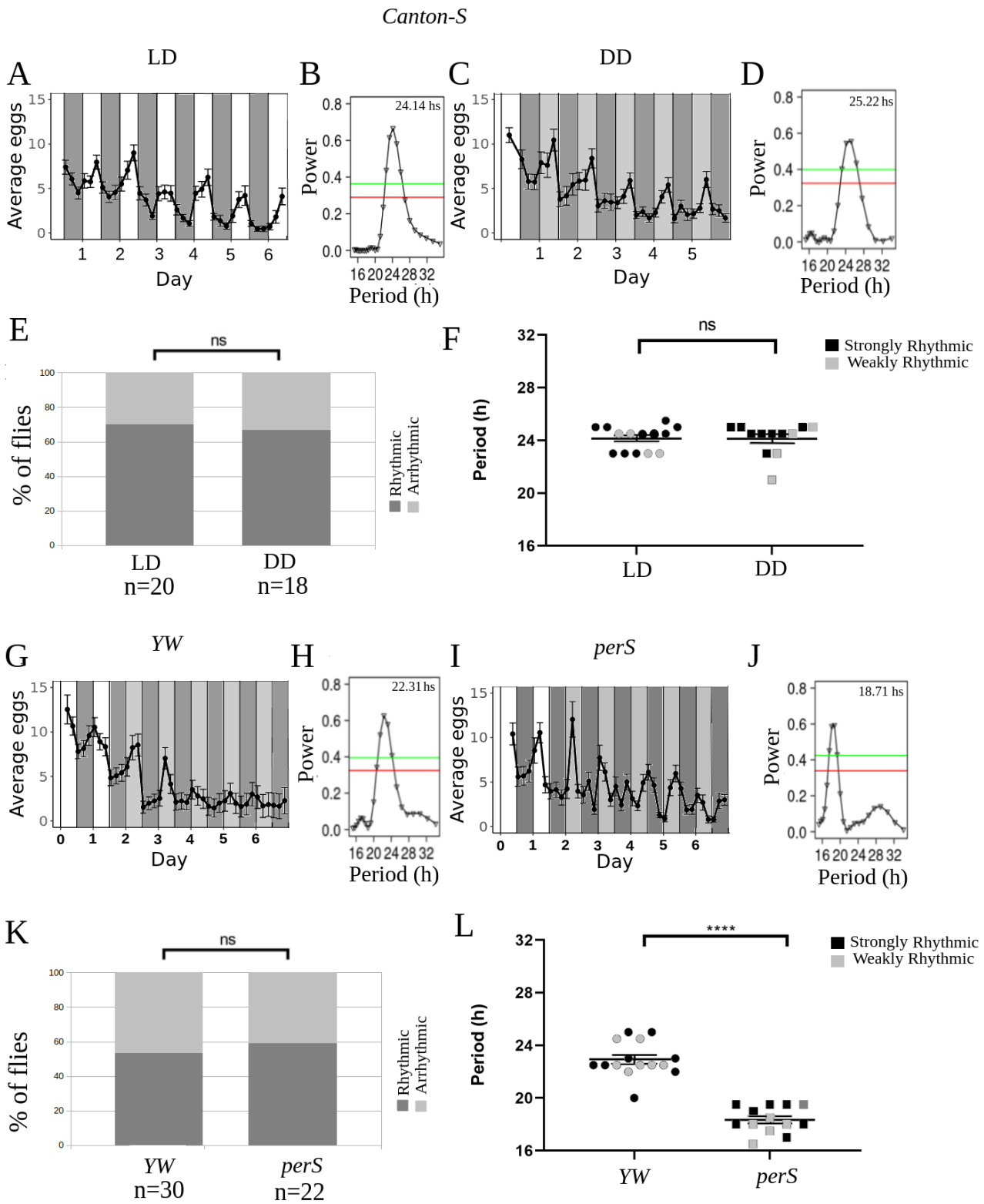

Figure 1. Oviposition in *Drosophila* is rhythmic when registered with our semiautomated egg collection device. A, C, G, I: Average eggs collected as a function of time in four different experiment (*Canton-S, LD*: A, Canton-S, DD:C; *YW*: G; *perS*: I). The average was made with all flies (Strongly rhythmic, weakly rhythmic and arrhythmic). White and dark grey bars represent periods of lights on and off respectively (LD), whereas light gray bars represent subjective days, DD, (i.e times where lights were on at rearing, but are now off). **B, D, H, J**: Lomb-Scargle periodograms of all genotypes, made with all flies, strongly rhythmic, weakly rhythmic and arrhythmic. Red and green horizontal

147 lines represent significances of 0.05 and 0.01, respectively. **E, K**: Percentage of females with rhythmic
148 oviposition (E: *Canton-S* in LD and DD, K: *YW* and p*erS*). The rhythmic flies include both strongly and
149 weakly rhythmic flies. **F, L**: Period of oviposition rhythms for rhythmic individual flies (F: *Canton-S* in
150 LD and DD, L: *YW* and *perS*). ns: non significant, ***p<0.001 (chi-squared test for scatter plots and
151 proportions).
152

153 **Downregulation of *per* in clock neurons causes a dramatic reduction in the power of egg-laying**
154 **rhythms.**

155 The circadian system of *Drosophila* comprises a central clock located in the brain that controls
156 locomotor behavior, as well as peripheral clocks located in many tissues, that regulate distinct
157 behaviors (Franco et al., 2018; Ito and Tomioka, 2016). For example, olfaction rhythms are controlled
158 by peripheral clocks in the antennae, and eclosion rhythms are partially controlled by peripheral
159 clocks in the prothoracic gland (Myers et al., 2003; Tanoue et al., 2004). Earlier work proposed that
160 oviposition might also be controlled by a peripheral clock (Manjunatha et al., 2008). In order to test
161 for this possibility, we used RNA interference (RNAi) to knock down the clock protein PER (Herrero
162 et al., 2017; Zhang et al., 2021) in all clock neurons in the brain (using the *Clk*856 driver (Gummadova
163 et al., 2009)), thereby disrupting their molecular clock. First, we tested the effectiveness of this tool
164 by monitoring the locomotor activity of males with their endogenous clock silenced in all clock
165 neurons (*Clk*856-Gal4>UAS-per^{RNAi}). **Supplementary Table 1** shows that these flies exhibited a
166 significant decrease in locomotor rhythmicity compared to their genetic controls. Having confirmed
167 the effectiveness of the RNA interference, we then monitored egg-laying in females from the
168 previously mentioned lines.

169 As shown in **Figure 2D,E**, when PER is knocked down in all clock neurons oviposition rhythmicity is
170 drastically reduced compared to controls **Figure 2B,C**. Notice, however, that the peak observed in
171 Fig. 2C has not disappeared completely in 2E, and is in fact not far from the significance threshold.
172 This could be due to some remaining rhythmicity in some individuals (although noise precludes the
173 observation of this at the individual level). Interestingly, when locomotor activity is studied in male

of this genotype, there is a fraction (less than 40%) of individuals that remain rhythmic in DD (see **Supplementary Table 1**).

This could be due either to the contribution of some peripheral oscillator/s relevant for the control of this behavior, or the presence of some residual PER in clock cells (Herrero et al., 2017).

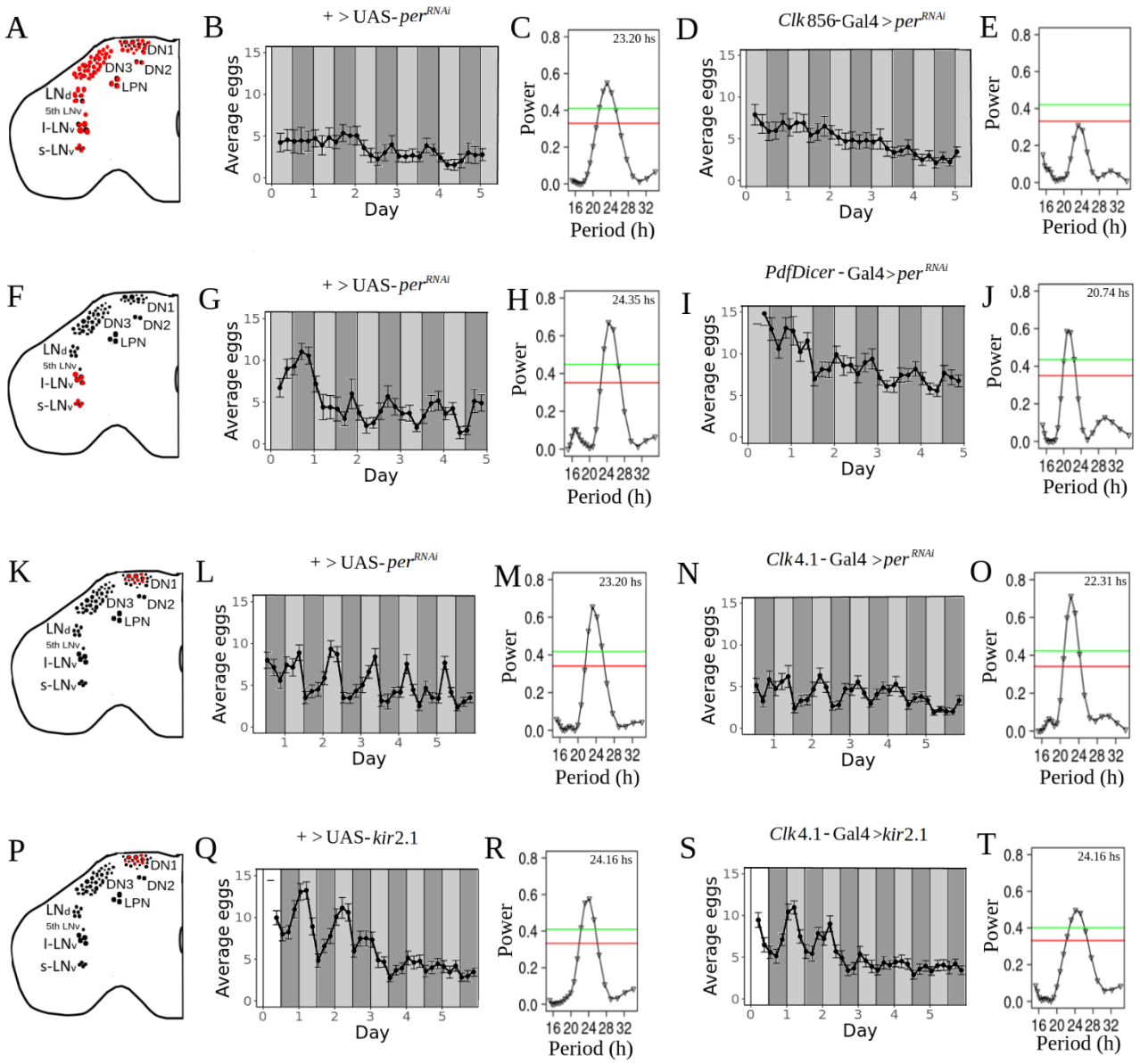

Figure 2. Circadian rhythmicity of oviposition is dramatically reduced when the molecular clock is disrupted in all clock neurons, but not when only LNv or DN1 neurons are affected. A, F, K, P: Schematic diagram of the neurons (painted in red) where the molecular clock has been disrupted. **B, D, G, I, L, N, Q, S**: Average eggs collected as a function of time. The average was made with all flies (strongly rhythmic, weakly rhythmic and arrhythmic). White and dark grey bars represent periods of lights on and off respectively (LD), whereas light gray bars represent subjective days, DD, (i.e times where lights were on at rearing, but are now off).**C, E, H, J, M, O, R, T**: Lomb-Scargle

187 periodograms of all genotypes (made with all flies, rhythmic, weakly rhythmic and arrhythmic). Red
188 and green horizontal lines represent significances of 0.05 and 0.01, respectively. **B, C**: +>UAS-*per*^{RNAi},
189 n=22. **D, E**: *Clk*856-Gal4>UAS-*per*^{RNAi}, n=26. **G, H**: +>UAS-*per*^{RNAi}, n=18. **I, J**: *PdfDicer*-Gal4>UAS-
190 *per*^{RNAi}, n=34. **L, M**:+>UAS-*per*^{RNAi}, n=38. **N, O**: *Clk*4.1-Gal4>UAS-*per*^{RNAi} , n=40. **Q, R**: +>UAS-*kir*2.1,
191 n=36. **S, T**:*Clk*4.1-Gal4>UAS-*kir*2.1, n=35.
192

193 **LNv and DN1 neurons are not necessary for egg-laying rhythmicity**

194 We next sought to establish the role of the most important circadian groups in the control of
195 oviposition. We concentrated on three groups: LNv, DN1p and LNd neurons. The LNvs are known to
196 be essential for the maintenance of circadian locomotor activity rhythms, and are the only ones that
197 express the PDF neuropeptide (Renn et al., 1999; Yoshii et al., 2009). However, we found that *per*^{RNAi}
198 mediated disruption of the molecular clock in PDF+ cells does not abolish the time-of-day dependent
199 oviposition (see **Figure 2G,H,I,J**). This is in line with previous results describing rhythmic oviposition
200 after ablation of all PDF+ neurons (Howlader et al., 2006a). In addition, we observed a shortening
201 of the egg-laying period when compared to controls, (20.74 h +/- 1.21 h vs 24.35 h+/-1.83 h
202 respectively, **Figure 2H,J**). This shortening can also be observed at the individual level
203 (**Supplementary Figure 2S1**). Taken together, these results suggest that these neurons may have
204 some influence on the control of this behavior.
205 The DN1 neurons are not essential for the maintenance of locomotor rhythms in DD, but they
206 contribute to the siesta (Guo et al., 2016) and generation of evening activity (Helfrich-Förster et al.,
207 2007; Zhang et al., 2010) when the peak of egg deposition occurs. Interestingly, it has recently been
208 shown that a posterior subset (DN1p) drives the circadian rhythm of oogenesis through the
209 neuropeptide allatostatin C (Zhang et al., 2021). To examine whether the molecular clock of DN1p
210 neurons is involved in the control of rhythmic oviposition, we evaluated the impact of PER
211 downregulation on mated females expressing the *Clk*4.1 driver (which is expressed in ~10 DN1ps per
212 hemisphere (Zhang et al., 2010)). As **Figure 2L,M,N,O** shows, the disruption of the clock in these
213 neurons does not alter the rhythmicity of egg-laying in DD. To further confirm these results, and in

214 the process examine if some other features of the DN1p could contribute to the control of
215 oviposition, we silenced these neurons through the expression of the inward rectifier potassium
216 channel *kir*2.1 (Baines et al., 2001). Silencing DN1p neurons did not affect the rhythmicity of egg-
217 laying in females which showed similar patterns to those exhibited by controls females (**Figures**
218 **2Q,R,S,T**). Taken together, these results show that neither LNv nor DN1p neurons play an important
219 role for rhythmic oviposition.
220

221 **The molecular clock in Cry+ LNd neurons is necessary for rhythmic egg-laying**

222 The LNd neurons include 6 cells whose expression pattern is very heterogeneous (Hermann-Luibl
223 and Helfrich-Förster, 2015; Ma et al., 2021). This group contains a subset of 3 Cry+ LNd neurons that
224 express both *cry* (which encodes the light sensing protein cryptochrome) and *pdfr* (the PDF
225 receptor), and 3 Cry- LNd neurons, that express neither of these genes (Im et al., 2011; Yoshii et al.,
226 2008). Even though the LNds are not essential for rhythmic locomotor activity under constant
227 conditions the Cry+ LNds, together with the 5-th sLNv, termed the "E oscillator", are the main drivers
228 of evening activity (Stoleru et al., 2004). These two LNd groups greatly differ in their connectivity to
229 the rest of the brain, since Cry+ LNds have both many more outputs and inputs than the Cry- LNds
230 (Shafer et al., 2022). In order to assess the role of the Cry+ LNds in the control of oviposition, we
231 employed a Gal4 driver, *Mai*179-Gal4; *pdf*-Gal80 (Grima et al., 2004; Picot et al., 2007), to direct
232 expression to E cells. This driver is expressed in the 5th sLNv, 3 Cry+ LNds, and also drives weak
233 expression in a small subset of DN1s. As **Figure 3 G** shows, impairing clock function in Cry+ LNds
234 results in a drastic reduction of rhythmic egg-laying compared with the genetic controls (**Figure 3 C,**
235 **E**). To further confirm this observation, we used another approach to disrupt the molecular clock in
236 those neurons, resorting to the very specific MB122B driver which is expressed in three LNds and
237 5th sLNv neurons (Duhart et al., 2020; Guo et al., 2017). We also used a different UAS sequence, a
238 dominant negative version of the clock gene *cycle* (Balaji Krishnan, 1999) . As expected, under these

239 conditions rhythmic egg laying was also severely compromised (**Figure 3M,N**), as compared with the
240 genetic controls (**Figure 3I,J,K,L**). Moreover, when we used RNAi to knock down the clock protein
241 PER with the MB122B driver, the results were very similar to those obtained with the Mai179-Gal4;
242 pdf-Gal80 driver (**Supplementary figure 3S1)**. Thus**,** we conclude that the molecular clock in Cry+
243 LNd neurons is necessary for the generation of egg-laying rhythms.
244 The appearance of two non-significant peaks in Figure 3 G (and Supp. Fig 3S1) might suggest that
245 these genetic manipulations of the LNds neurons generate weakened complex rhythms (Beckwith
246 and Ceriani, 2015) instead of complete arrhythmicity. This would mean that, at the individual level,
247 there should be either many flies with a corresponding complex rhythm, or two weakly rhythmic
248 subpopulations, each one accounting for one of the peaks of the average periodogram. However, an
249 examination of the individual periodograms (Supplementary Figures 3S2 to 3S7) does not provide
250 convincing evidence to support any of these two hypotheses. On the other hand, when the method
251 is applied to synthetic, completely random time series, it can generate periodograms with two non
252 significant peaks (as shown in panels **2,3, and 4 of Figure S12 of the Supplementary Material**). Thus,
253 we favor the hypothesis that the two peaks present in Figure 3 G (and **Supplementary Figure 3S1**)
254 are spurious.
255 It has recently been shown that disrupting the molecular clock in E cells by means of the MB122B
256 driver did not alter locomotor activity rhythms (Bulthuis et al., 2019). This would imply that
257 locomotor activity and oviposition rhythms are controlled by distinct groups of clock neurons.
258 However, Bulthuis et al. (2019) only assessed the locomotor activity of male flies, and it is well known
259 that, unlike males, females undergo important changes in their activity after mating, such as the loss
260 of the midday siesta (Elwyn Isaac et al., 2010) or the morning anticipation (Riva et al., 2022). For
261 these reasons, we decided to examine the influence of the molecular clock of E cells directly on the
262 locomotor activity of mated females. The standard setup for assessing locomotor activity is the
263 Drosophila Activity Monitoring (DAM) system (Pfeiffenberger et al., 2010), where flies are housed in

small glass tubes (of 5mm in diameter). Such arena does not offer an adequate environment for testing flies that lay eggs during several days; instead, we monitored activity using an alternative system developed in our lab, where flies are housed in much larger cubicles and their activity is recorded by a video system (see Methods and (Riva et al., 2022)). Interestingly, mated females with disrupted E cell clocks were as rhythmic as control flies (**Figure 4**), showing that there is no sex-specific contribution of this cluster to the control of rhythmic rest-activity cycles, which opens the possibility that E cells differently contribute to the control of oviposition and locomotor activity. In other words, our results show that these two important rhythmic behaviors are primarily controlled by distinct groups of clock neurons.

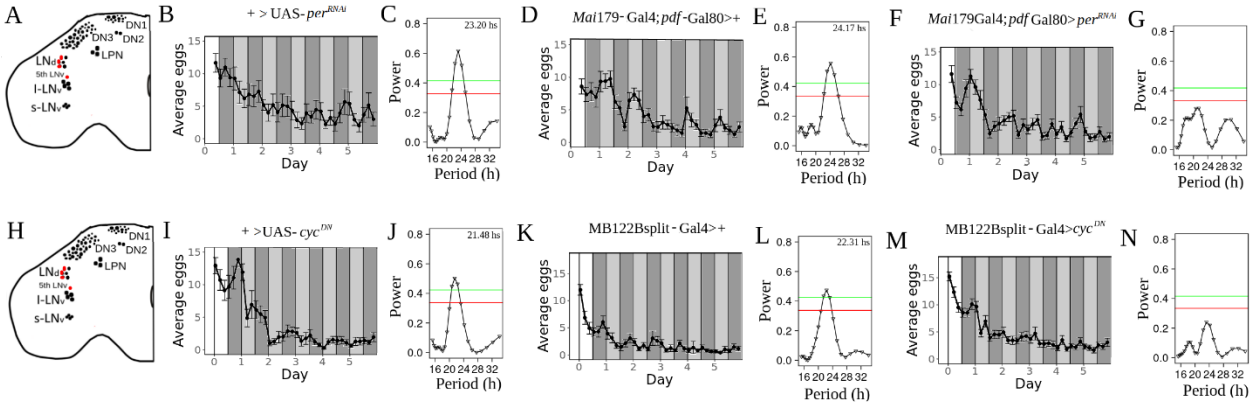

Figure 3. Disruption of the molecular clock in Cry+ LNd neurons drastically reduces the circadian rhythmicity of oviposition. A, H: Schematic diagram of the neurons (painted in red) where the molecular clocks have been disrupted. **B, D, F, I, K, M**: Average eggs collected as a function of time. The average was made with all flies (Strongly rhythmic, weakly rhythmic and arrhythmic). White and dark grey bars represent periods of lights on and off respectively (LD), whereas light gray bars represent subjective days, DD, (i.e times where lights were on at rearing, but are now off).**C, E, G, J, L, N**: Lomb-Scargle periodograms of all genotypes (made with all flies, rhythmic, weakly rhythmic and arrhythmic). Red and green horizontal lines represent significances of 0.05 and 0.01, respectively. **B, C**: +>UAS-*per*^{RNAi}, n= 15. **D, E**: *Mai*179-Gal4;*pdf*-Gal80>+, n= 17. **F, G**: *Mai*179-Gal4;*pdf*-Gal80>UAS-*per*^{RNAi}, n=28. **I, J**: +>UAS-*cyc*^{DN}, n=15. **K, L**: MB122Bsplit-Gal4>+, n=14. **M, N**: MB122Bsplit-Gal4>UAS-*cyc*^{DN} , n=30.

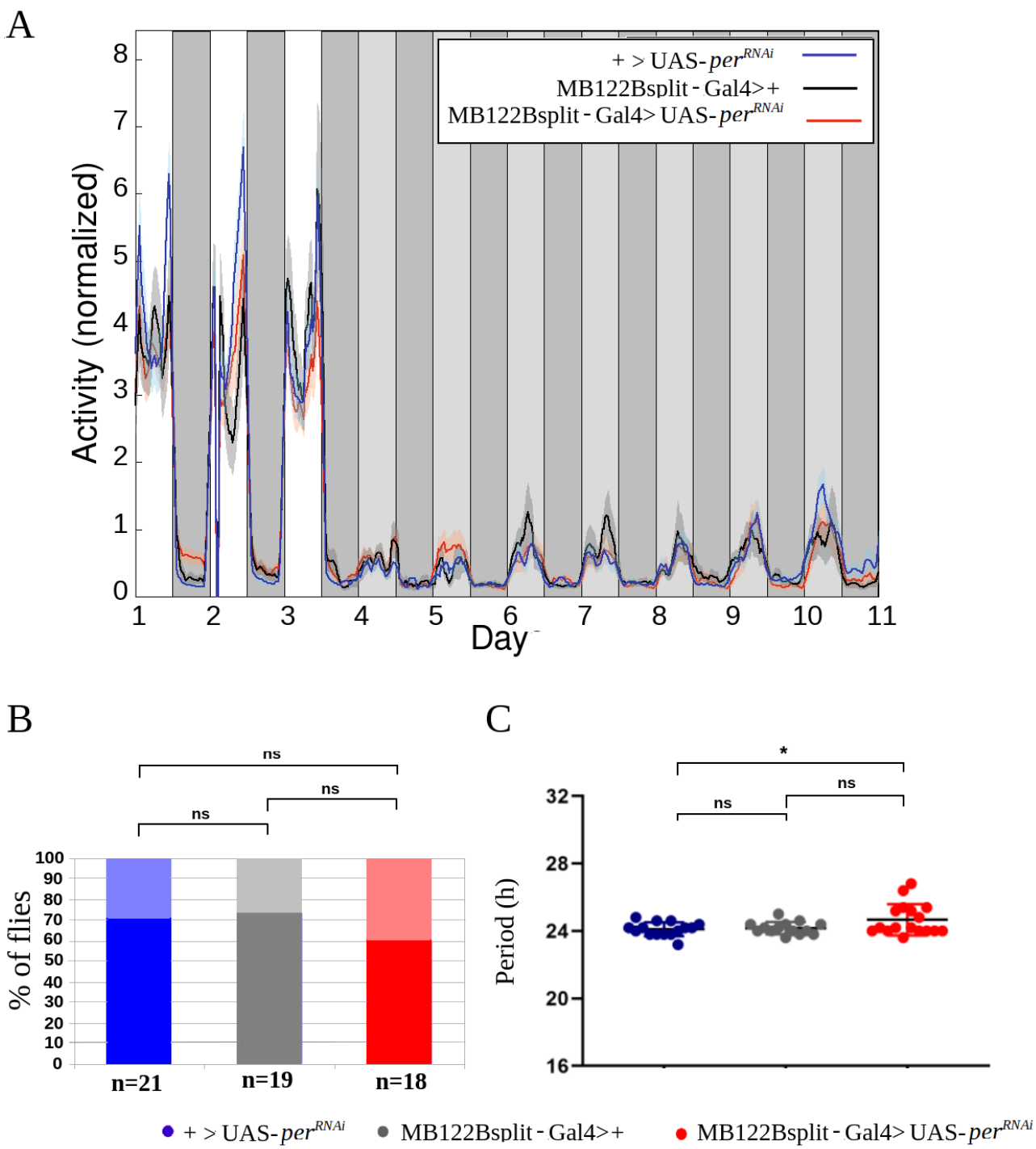

Figure 4. Disruption of the molecular clock in Cry+ LNd neurons does not alter the circadian rhythmicity of locomotor activity of mated female flies. A: Average activity recording during 3 days in LD and 7 in DD. Light grey bars represent subjective days. **B**: Percent of rhythmic flies in DD. **C**: Periods of locomotor activity in DD of individually rhythmic flies. Mean ± SEM indicated. Each dot represents one fly. ns: non significant, *: p<0.05 (chi-squared test for the comparison of proportions , and one-way-ANOVA with post-hoc Tukey for the scatter plots.

Cry+ LNd neurons directly contact oviIN

294 If the circadian clock influences oviposition, at least some clock neurons should be connected,
295 directly or indirectly, to the neurons in the brain that control the motor program leading to egg
296 deposition. These neurons, that were recently characterized (Vijayan et al., 2023a; Wang et al., 2020;
297 Zhou et al., 2014), include: the oviposition descending neurons (oviDN, 5 per hemisphere), the
298 oviposition excitatory neurons (oviEN, 1 per hemisphere), the oviposition inhibitory neurons (oviIN,
299 1 per hemisphere), and pC1 neurons (5 per hemisphere). The best tool in hand to systematically
300 probe the connectivity between circadian clock and oviposition-related neurons is the *Drosophila*
301 hemibrain connectome (Scheffer et al., 2020). This is the result of the FlyEM connectomics project,
302 which used electron microscopy images of the brain of a 5-day old female fly to reconstruct the
303 connectivity map (or connectome) of ~25000 neurons, mostly from the central part and the right
304 lateral part of the brain.
305 28 of these neurons have been identified as clock neurons, and are located in the right part of the
306 brain (except for one LPN (Scheffer et al., 2020)). These include the best characterized circadian
307 groups (sLNvs, lLNvs, LNds). For other groups, such as the DN1s and LPNs, only a minor fraction have
308 been identified, whereas for groups DN2 and DN3 no neurons have yet been identified in this
309 volume.
310 Interestingly, almost all oviposition-related neurons have been identified in the hemibrain (only two
311 oviDN on the left hemisphere are still missing), and very recently a couple of additional groups called
312 U and G, comprising 2 and 5 neurons each, respectively, have also been shown to be important for
313 oviposition and mapped to the connectome (Vijayan et al., 2023b). This makes a total of 25
314 oviposition-related neurons identified thus far.
315 To address the possibility of direct connections between clock neurons and neurons involved in egg
316 laying, we probed the hemibrain connectome for these connections. The full results are displayed in
317 **Supplementary Tables 2 and 3**, but in short, we found that whereas there are no connections
318 between LNv or DN1 neurons and oviposition neurons, LNds contact oviIN and pC1 neurons (**Figure**

5), further supporting the experimental findings described in previous sections. Interestingly, different subgroups of E cells (Shafer et al., 2022) show distinct patterns of connectivity to oviposition neurons: E3 neurons (comprising Cry- LNd1, LNd2 and LNd3) only contact the pC1 group, while E2 neurons (comprising Cry+ LNd4 and LNd5) only contact the oviIN neurons (**Figure 5**). On the other hand, the E1 neurons (comprising Cry+ LNd6 and 5-th sLNv) make no contacts with oviposition related neurons. This evidence suggests that the subset of E cells responsible for the loss of rhythmic oviposition are likely E2 neurons.

Interestingly, we noticed that connections between clock and oviposition neurons are bidirectional, although the E2-oviIN connection is stronger in the direction from the clock to oviposition neurons. This analysis suggests that, even though some feedback is anticipated, the E2 neurons are likely the ones providing temporal information to the oviposition circuit.

Additionally, aside from the circadian groups considered so far, we found strong, bidirectional connections between the clock neurons LPN (Reinhard et al., 2022) and the oviIN, with the strongest connections going from oviIN to LPN (**Supplementary Tables 2 and 3 and Supplementary Figure 5S1**).

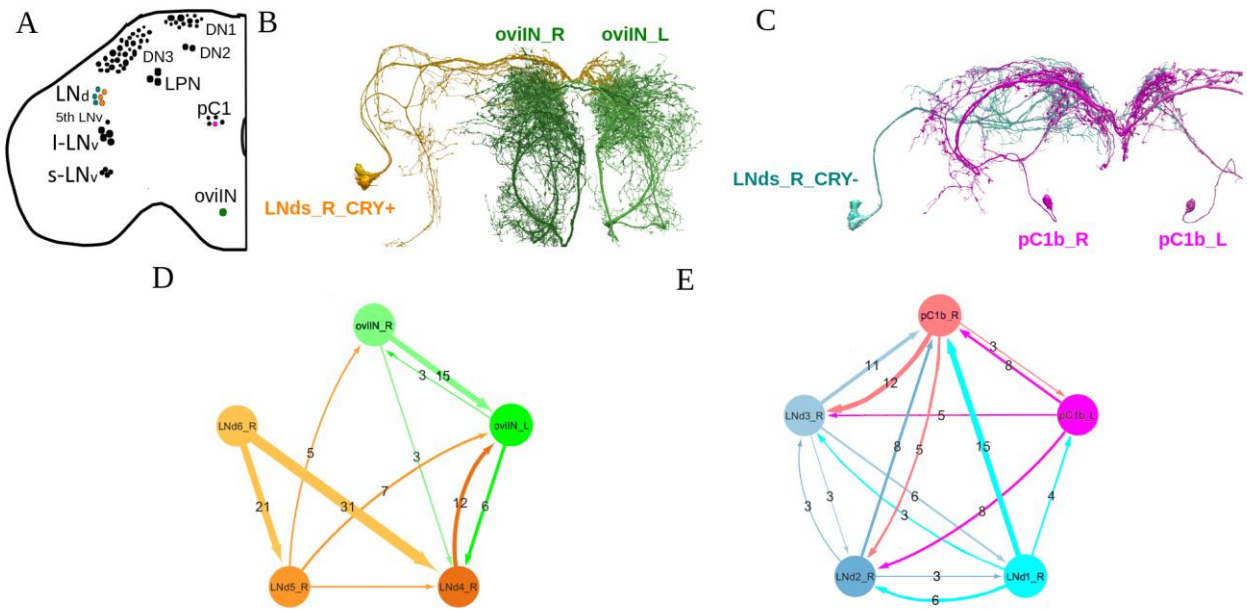

Figure 5. Direct synaptic connections between circadian clock neurons and oviposition-related neurons in the hemibrain dataset. A: Schematic diagrams showing the different neuron clusters analyzed (in color). **B**: Connection between Cry+ LNd and oviIN neurons. **C**: Connection between Cry- LNd 2and pC1b neurons. **D**: Network representation of the connectivity between Cry+ LNd and oviIN neurons. **E**: Network representation of the connectivity between Cry- LNd and pC1b neurons. Numbers give the number of synaptic contacts, which represent the strength of the connections. Only intermediate (between 3 and 9 synaptic contacts) and strong (>9 synaptic contacts) connections are considered.

DISCUSSION

The oviposition rhythm is one of the less studied behavioral traits of *Drosophila*. One possible reason is merely technical, since egg collection and counting are a very laborious processes and there are no standard devices (just as the DAM system for locomotor activity) to reproducibly evaluate it. Data analysis and rhythmicity assessments are also particularly difficult because the presence or absence of a rhythm must be established with only approximately 6 data points per cycle (in contrast to locomotor activity time series, where hundreds of data points per cycle are obtained), which can take only a few discrete values (typically, from 0 to 10). The analysis is further complicated by the fact that the daily average of eggs laid decreases with time (Kaufman and Demerec, 1942). To tackle these limitations, we developed a semiautomated method for egg collection and a new pipeline for data analysis. We observed that the oviposition rhythm is less consolidated than locomotor activity rhythms. Surprisingly, this happens even in LD, where time of day cues are provided by light, the most important *zeitgeber* for diurnal animals. Egg-laying is even less rhythmic in DD since the information from the endogenous clock is one among many internal and external factors that influence the decision of laying an egg. In a sense, the oviposition record of a single fly can be considered as periodic signal with strong noise added to it. Such data might not even look rhythmic when analyzed individually. However, if we assume that the periodic component is the same for all flies in a population, and the noise is different for each individual, the periodic component can be extracted by averaging the oviposition data. This led us to prefer periodograms of averaged data for the assessment of the rhythmicity of a given genotype.

365 Even though there have been some advances in the understanding of the relationship between
366 circadian clock and oviposition (Howlader and Sharma, 2006; Manjunatha et al., 2008), there is still
367 no information about the relative importance of the different neuronal groups in driving this
368 behavior. Here, we downregulated the molecular clock in subsets of circadian neurons in order to
369 establish their role in the control of circadian oviposition. First, we found that animals with
370 downregulated *per* expression in all clock neurons of the brain display a drastic reduction of rhythmic
371 oviposition, underscoring a key role of the central clock (as compared with peripheral clocks) in the
372 control of the timing of oviposition.
373 Even though we also disrupted the molecular clock in PDF-expressing neurons as well as in the DN1p
374 group, egg-laying rhythms were not abolished, in agreement with previous reports (Howlader et al.,
375 2006a). We cannot rule out a contribution of PDF-expressing neurons, since we observed a
376 shortening of the oviposition period. Interestingly, a previous work (Howlader et al., 2006b) reported
377 a similar period shortening in pdf^{01} mutant flies, but not when PDF-expressing neurons were ablated.
378 Taken together, these results show that communication between either group and any other
379 neurons is not necessary for rhythmic oviposition. This is in stark contrast with the situation for
380 locomotor activity, which has been shown to become arrhythmic when PDF+ cells are ablated
381 (Grima et al., 2004; Stoleru et al., 2004). Interestingly, however, it has been recently shown that
382 disrupting the molecular clock in these same neurons does not alter locomotor rhythmicity
383 (Delventhal et al., 2019; Schlichting et al., 2019) suggesting a more complex scenario.
384 Since it has been shown that the DN1p generate the rhythm of oogenesis (Zhang et al., 2021), one
385 might wonder why the disruption of their molecular clock or their electrical silencing does not also
386 abolish the rhythm of oviposition. It is important to understand that the suppression of the
387 oogenesis rhythm does not necessarily have an impact on rhythmic egg laying. The persistence of
388 oviposition rhythm suggests that it does not depend on the rhythmic production of oocytes, but is

389 instead an intrinsic property of the motor program which is the hypothesis more supported by our
390 results.
391 Somewhat surprisingly, the disruption of the molecular clock in Cry + LNd neurons led to an almost
392 complete loss of the oviposition rhythm. In contrast, downregulating the clock in Cry+ LNds did not
393 affect rhythmic locomotor activity in mated females, underscoring a degree of specificity.
394 Interestingly, in males the Cry+ LNds have been singled out as responsible for driving the activity
395 peak at dusk (evening peak, (Guo et al., 2017)), which is the time when, in females, egg laying has a
396 peak. As far as we know, oviposition is the first female-specific behaviour specifically controlled by
397 the LNds. In males the LNds have been shown to be involved in the circadian control of the
398 expression of sex-specific fat body genes (Erion et al., 2016; Fujii et al., 2008).
399 The neural circuitry that controls the egg laying process has just begun to be unraveled (Vijayan et
400 al., 2023a; Wang et al., 2020; Zhou et al., 2014). It includes the oviDNs, oviINs, oviENs, groups U and
401 G, and pC1 neurons. Using the hemibrain connectome we found that neither the identified DN1s
402 nor the LNv neurons directly contact any neurons ascribed to the oviposition circuit; the LNd cluster,
403 on the other hand, exhibits synaptic contacts with pC1 and oviIN neurons, providing the anatomical
404 substrate for our experimental results. Furthermore, there is a clear separation of roles inside the
405 LNd cluster, since the oviINs are only contacted by two Cry+ LNds (the so-called E2 cells (Shafer et
406 al., 2022)) and the pC1s are only contacted by the three Cry- LNds (E3 cells (Shafer et al., 2022)).
407 There is also a functional separation within the pC1 cluster, since the only pC1 neurons connected
408 E3 neurons are the pC1b neurons from both right and left hemispheres (**Figure 5**). The resulting
409 clock/oviposition network is summarized in **Figure 6**.

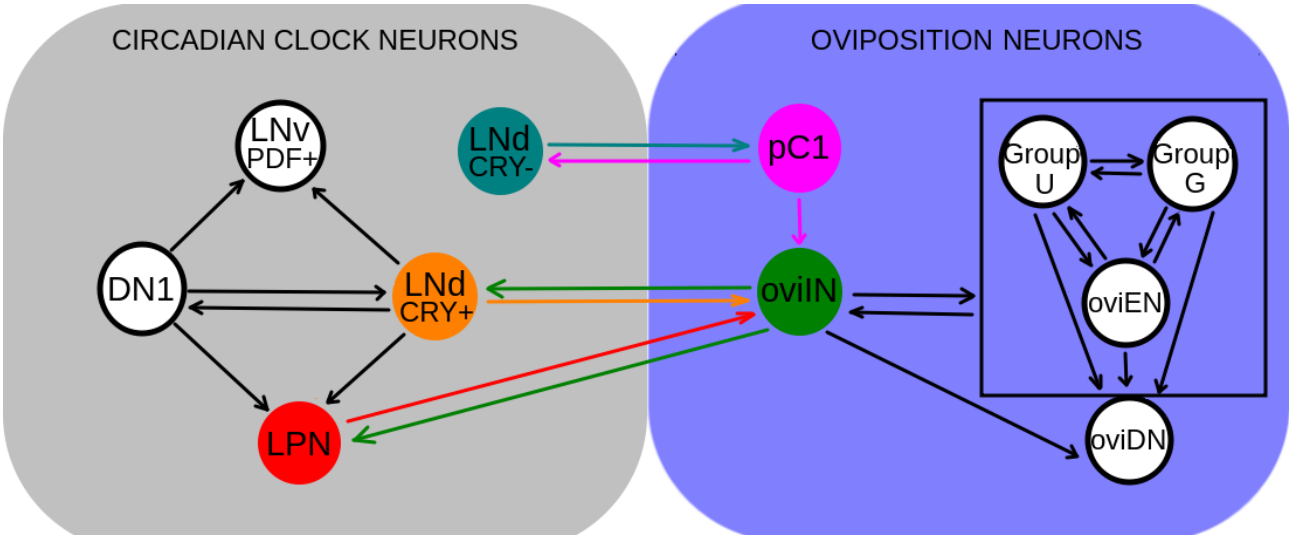

Figure 6. Scheme of connections between circadian clock and oviposition-related neuron clusters of the same hemisphere in the hemibrain dataset. Each circle represents a neuron cluster, comprising different numbers of neurons (some clusters comprise only one neuron). Clusters and connections involved in the connectivity between circadian clock and oviposition sets have been colored. In each connection the arrow points to the post-synaptic cluster. OviIN neurons are bidirectionally connected to every neuron of the clusters inside the square.

Our data posits the E2 LNds-oviIN connection as the candidate to mediate the timing of egg laying rhythms. The oviIN neurons are two of the most important neuronal hubs included in the current version of the *Drosophila* connectome, receiving strong inputs of hundreds of other neurons. Thus, the oviINs integrate the information from the circadian clock with the information coming from many other sources in order to signal to the oviposition circuit. Under such scenario the circadian clock would compete with many other sources to set the threshold for egg deposition (Vijayan et al., 2023a).

We hypothesize that the E3-pC1b connection is less important for conveying circadian information to the oviposition circuit because the pC1b are located upstream within the oviposition circuit that controls the motor program, being connected only to the oviIN neurons (Wang et al., 2020). On the other hand, since pC1 neurons control female receptivity, it is tempting to speculate that this behavior may have a circadian rhythm, that could be generated through the E3-pC1b connection. Interestingly, the female mating rate has been shown to display circadian rhythmicity (Sakai and

431 Ishida, 2001), and very recently it has been proposed that pC1b neurons are involved in the control
432 of female copulation rate (Li et al., 2023). Conversely, given that the E3-pC1b connection is
433 bidirectional, it could also be instrumental in conveying information about mating status to the
434 circadian clock, therefore producing the changes in temporal organization that females undergo
435 after mating (Delbare et al., 2023; Elwyn Isaac et al., 2010; Riva et al., 2022).
436 The function of the LPN neurons in the circadian clock is still unclear (Reinhard et al., 2022) and
437 therefore no clear role in rhythmic oviposition can be ascribed to the LPN-oviIN connection. On the
438 other hand, since there are many more oviIN inputs to the LPN than outputs (135 vs 16 synaptic
439 connections), it seems more likely that this connection conveys information to the circadian clock
440 from those processes in which the oviINs are involved.
441 The information provided by the *Drosophila* connectome is only the first step towards the
442 understanding of the influence of the circadian clock on oviposition. Future work will be necessary
443 to test the functionality of these connections as well as the role of different neuropeptides (sNPF,
444 ITP, PDF) and neurotransmitters (such as acetylcholine and glutamate) in the control of egg laying
445 behavior.
446
447
448 **MATERIAL AND METHODS**
449 **Fly strains**
450 All fly strains used in this study are detailed in Table 1. Flies were reared and maintained on standard
451 cornmeal/agar medium at 25 °C and 60% humidity in a 12 hr:12 hr LD cycle unless stated otherwise.
452 For oviposition and locomotor activity experiments we used a different medium, named banana
453 medium, prepared with 200g of banana, 25g of barley, 36g of black sugar, 35 g of yeast, 12.5g of
454 agar and 2g of Nipagin per liter of water.
455

456 **Table 1**

457 All fly strains used in this study.

***Drosophila melanogaster* line**	**Source**	**Identification number**	**Common denomination**
Canton-S	*Bloomington Drosophila Stock Center*	BDSC: 64349	*CS*
Yellow white	*Bloomington Drosophila Stock Center*	BDSC: 1495	*y w*
y perS w	Donated by Jeff Hall	Collection of Jeff Hall	per^{S}
y[1] sc[*] v[1] sev[21]; P{y[+t7.7] v[+t1.8]=TRiP.HMS 02045}attP2/TM3, Sb[1]	*Bloomington Drosophila Stock Center*	BDSC:40878	UAS-per^{RNAi}
w[*]; P{w[+mC]=Clk-GAL4.-856}2	*Bloomington Drosophila Stock Center*	BDSC:93198	*Clk856*-Gal4
w[*]; sna[Sco]/CyO; P{w[+mC]=Clk-GAL4.1.5}4.1M/TM	*Bloomington Drosophila Stock Center*	BDSC:36316	*Clk*4.1-Gal4

6B, Tb[1]			
P{w[+mC]=Pdf-GAL4.P2.4}X, y[1] w[*];Dicer/cyo	*Bloomington Drosophila Stock Center*	BDSC:6899	*PdfDicer*-Gal4
*Mai*179-Gal4;*Pdf*-Gal80	Donated by José Duhart	Collection of Patrick Emery	*Mai179-Gal4;Pdf-Gal80*
MB122B E-cell split-Gal4	Donated by José Duhart	Collection of Orie Shafer	*MB122B*-splitGal4
w;; kir2.1(1)/TM3 Sb	Donated by Justin Blau	Collection of Justin Blau	UAS-*kir*2.1
w;UAS-cyc^{DN};+	Donated by Fernanda Ceriani	Collection of Sebastian Kadener	UAS-cyc^{DN}

458

459 **Semiautomated egg collection device**

460 The egg collection device (Supplementary **Figure 1 S1** and **supplementary video**) consists of a
461 wooden basis with a mechanical arm fixed to it, and plastic sets of tracks with fly chambers that can
462 be replaced at will. Each "set of tracks" is a 13.9 x 19.5 cm 3D-printed piece with 7 tracks. Inside each
463 track there are 6 equidistant wells measuring 15 x 20 mm, which are filled with banana medium.
464 Each fly chamber (17 x 27 mm) has a transparent roof, and no floor, so that the fly inside it is in
465 contact with the food wells, when the chamber is placed on the track so that it can slide along it. 3

466 sets of tracks are placed on the wooden base, and the chambers are moved together from well to
467 well by a mechanical arm, which is moved by a stepper motor controlled by an Arduino UNO. The
468 chambers are displaced from well to well every 4 hours. More frequent sampling gives rise to less
469 consistent rhythmic patterns. Survival in this egg collection device is in general high: on average,
470 more than 80% of the flies are alive at the end of an egg collection experiment lasting one week.

471 **Behavioral assays**

472 The egg deposition behavior of females was analyzed individually at 25°C and 60% humidity. Before
473 starting the assay, six 0-5 day old virgin females and five males of the desired genotype were
474 anesthetized using CO_2 and introduced into a vial with 10mL of standard food for 72 hours. This
475 allowed for the crossing of 50-80 female flies with their respective males per experiment.
476 Subsequently, the resulting gravid females from the crosses were placed individually in vials
477 containing a plastic spoon with 1.5mL banana medium along with a drop of yeast for one day. The
478 eggs deposited by each of the females are counted under a binocular stereoscopic magnifier (Lancet
479 Instruments) and the 21 best egg layers are selected to conduct the circadian oviposition
480 experiment. This prior selection of the best egg layers is performed because, of the total females put
481 to mate with males, nearly half do not lay eggs or lay very few.

482 21 of these females were housed in the chambers of each apparatus, which was then introduced in
483 an incubator at constant temperature (25 °C). The first 1 or 2 days the light regime was LD (12:12) in
484 order for the flies to adapt to their new environment, and then they entered a DD regime for a given
485 number of days. The sets of tracks were retired and replaced by sets with new food every 20, 24 or
486 28 hours (in order to avoid providing an entrainment signal to the flies). The eggs in each food well
487 of each of the retired tracks were counted under a binocular stereoscopic magnifier (Lancet
488 Instruments), and registered.

489 For the locomotor activity assays we used the setup used in previous works (Riva et al., 2022).
490 Briefly, the flies are housed in translucid tracks and their movement is registered with video cameras

above the tracks, connected to a computer, where the position of each fly is extracted from the video (with ad hoc programmed software) and registered. Locomotor activity of mated females was monitored for 3 days in LD conditions and then transferred to DD conditions for 7 days. Every 4 or 5 days the flies were transferred to tracks with fresh food, because after that time the appearance of larvae hindered the video tracking of the females.

Data analysis

After each oviposition experiment lasting N days the data consisted of a time series *E* of 6N points for each fly. A new time series was generated by averaging the individual series. Since the number of eggs laid by a mated female tend to show a downward trend, we proceeded as follows, in order to detrend the data (see the Supplementary Material for further details). First, a moving average of the data is performed, with a 6 point window, and a new time series *T* is obtained. In principle, *T* is a good approximation to the trend of the data. Then, a new, detrended, time series *D* is generated by pointwise dividing the two series (i.e. $D(i)=E(i)/T(i)$, where *i* indexes the points of each series).

In order to assess the rhythmicity of a genotype, we averaged the detrended time series and performed a Lomb-Scargle periodogram (Ruf, 1999; VanderPlas, 2018). For this we used package Lomb (version 2.1.0), from the R Statistical Software (v4.1.2; R Core Team 2021). The significance lines were calculated by repeatedly randomizing the time series (using function *randslp* in Lomb R package). A genotype was considered rhythmic if the periodogram had one peak between 16 and 32 hs, and it was above the p=0.05 significance line.

The graphs showing individual periods were made by obtaining the individual periods using the Lomb-Scargle periodogram described above for each particular individual. For the individual periods shown in the figures, we added the weakly rhythmic category, corresponding to flies whose periodograms displayed only one peak between 18 and 32 hs, and a power larger than 0.2.

More details about the method used can be found in the Supplementary Material.

516 For locomotor activity experiments, these files obtained from the video tracking were processed
517 with an analysis software we developed (in Bash) which provides statistics for activity (position,
518 distance traveled, etc.) (Riva et al., 2022).
519
520 **Analysis of connectome data**
521 The data used to determine the connectivity between the circadian clock and the oviposition circuits
522 come from the Hemibrain dataset (version 1.2.1) made publicly available by Janelia Research
523 Campus (Scheffer et al., 2020). To access the data we used the NeuPrintExplorer Web tool
524 (https://neuprint.janelia.org/). The result of our queries is summarized in **Supplementary Tables 2**
525 and **Table 3**. The neuron IDs are as given in the hemibrain dataset, just as the instance names of the
526 oviposition related neurons. For circadian clock neurons we used the names given by Shafer et al.
527 (Shafer et al., 2022). We only replaced LPN-4 by LPN-L to stress the fact that this neuron is placed in
528 the left hemisphere (all the others are in the right hemisphere). The strength of each connection
529 was quantified using the criteria of Scheffer et al. (Scheffer et al., 2020). Connections with more than
530 9 synapses were considered strong, connections having between 3 and 9 synapses were considered
531 as having intermediate strength, and connections with 0,1, or 2 synapses were considered as weak.
532 Because weak connections are prone to error (Scheffer et al., 2020) we excluded them from the
533 analyses. The figures that show connectivity between sets of neurons were drawn using Cytoscape
534 version 3.10.1 (Shannon et al., 2003).
535
536 **Statistical analysis**
537 The following statistical analyses were used for the comparison between genotypes of individual
538 periods (scatter plots). First, we tested data for normality with D'Agostino & Pearson test. Once the
539 normality of the data was confirmed, we used a unpaired t-test for test differences between means
540 for experiments where 2 groups were compared and a one-way ANOVA for experiments where 3

541 groups were compared. When data was not normally distributed, we applied a Mann-Whitney test
542 for test differences between means. When significant differences were found, we conducted a post-
543 hoc Tukey test with a correction for multiple comparisons. In all the analyses we used Two-Tailed *p*-
544 values. To perform all the tests, we used GraphPad Prism (Boston, Massachusetts USA,
545 www.graphpad.com) and R Statistical Software (v4.1.2; R Core Team 2021). $p < 0.05$ was considered
546 statistically significant. In dot plots, horizontal lines represent the mean value; error bars depict the
547 standard error of the mean. For the comparison between genotypes of the proportion of rhythmic
548 individuals over the total (proportion plots), we used the 'N-1' Chi-squared test as recommended by
549 Campbell (2007) (Campbell, 2007) and Richardson (2011) (Richardson, 2011). To perform these
550 tests, we use MedCalc Software Ltd. Comparison of proportions calculator (https://www.med-
551 calc.org/calc/comparison_of_proportions.php (Version 23.2.7; accessed June 19, 2025). No sta-
552 tistical methods were used to determine sample size. Sample sizes are similar to those generally
553 used in this field of research. Samples were not randomized and analyzers were not blind to the
554 experimental conditions. In all the figures we show results of two or three independent experi-
555 ments.

556

557 **REFERENCES**

558 Allada R, Emery P, Takahashi JS, Rosbash M. 2001. Stopping time: the genetics of fly and mouse
559 circadian clocks. Annual review of neuroscience **24**:1091–1119. DOI:
560 https://doi.org/10.1146/annurev.neuro.24.1.1091, PMID: 11520929
561 Allemand R. 1976. Les rythmes de vitellogenese et d'ovulation en photoperiode LD 12:12 de
562 Drosophila melanogaster. Journal of Insect Physiology **22**:1031–1035. DOI:
563 https://doi.org/https://doi.org/10.1016/0022-1910(76)90088-3
564 Bailly TPM, Kohlmeier P, Etienne RS, Wertheim B, Billeter JC. 2023. Social modulation of
565 oogenesis and egg laying in Drosophila melanogaster. Current Biology **33**:2865-2877.e4. DOI:
566 https://doi.org/10.1016/j.cub.2023.05.074, PMID: 37369209
567 Baines RA, Uhler JP, Thompson A, Sweeney ST, Bate M. 2001. Altered electrical properties in
568 Drosophila neurons developing without synaptic transmission. The Journal of neuroscience :
569 the official journal of the Society for Neuroscience **21**:1523–1531. DOI:
570 https://doi.org/10.1523/JNEUROSCI.21-05-01523.2001, PMID: 11222642
571 Balaji Krishnan SED& PEH. 1999. krishnan1999.
572 Beckwith EJ, Ceriani MF. 2015. Experimental assessment of the network properties of the
573 Drosophila circadian clock. Journal of Comparative Neurology **523**:982–996. DOI:

https://doi.org/10.1002/cne.23728, PMID: 25504089

Bulthuis N, Spontak KR, Kleeman B, Cavanaugh DJ. 2019. Neuronal Activity in Non-LNv Clock Cells Is Required to Produce Free-Running Rest:Activity Rhythms in Drosophila. Journal of Biological Rhythms **34**:249–271. DOI: https://doi.org/10.1177/0748730419841468, PMID: 30994046

Campbell I. 2007. Chi-squared and Fisher-Irwin tests of two-by-two tables with small sample recommendations. Statistics in Medicine **26**:3661–3675. DOI: https://doi.org/10.1002/sim.2832, PMID: 17315184

Cury KM, Prud'homme B, Gompel N. 2019. A short guide to insect oviposition: when, where and how to lay an egg. Journal of Neurogenetics **33**:75–89. DOI: https://doi.org/10.1080/01677063.2019.1586898, PMID: 31164023

Delbare SYN, Venkatraman S, Scuderi K, Wells MT, Wolfner MF, Basu S, Clark AG. 2023. Time series transcriptome analysis implicates the circadian clock in the Drosophila melanogaster female's response to sex peptide. Proceedings of the National Academy of Sciences of the United States of America **120**:e2214883120. DOI: https://doi.org/10.1073/pnas.2214883120, PMID: 36706221

Delventhal R, Pantalia M, O'Connor R, Ulgherait M, Kim H, Basturk M, Canman J, Shirasu-Hiza M. 2019. Dissection of central clock function in Drosophila through cell-specific CRISPR-mediated clock gene disruption. bioRxiv 640011. DOI: https://doi.org/10.1101/640011

Deppisch P, Prutscher JM, Pegoraro M, Tauber E, Wegener C, Helfrich-Förster C. 2022. Adaptation of Drosophila melanogaster to Long Photoperiods of High-Latitude Summers Is Facilitated by the ls-Timeless Allele. Journal of Biological Rhythms **37**:185–201. DOI: https://doi.org/10.1177/07487304221082448, PMID: 35301885

Duhart JM, Herrero A, de la Cruz G, Ispizua JI, Pírez N, Ceriani MF. 2020. Circadian Structural Plasticity Drives Remodeling of E Cell Output. Current Biology **30**:5040-5048.e5. DOI: https://doi.org/10.1016/j.cub.2020.09.057, PMID: 33065014

Elwyn Isaac R, Li C, Leedale AE, Shirras AD. 2010. Drosophila male sex peptide inhibits siesta sleep and promotes locomotor activity in the post-mated female. Proceedings of the Royal Society B: Biological Sciences **277**:65–70. DOI: https://doi.org/10.1098/rspb.2009.1236, PMID: 19793753

Erion R, King AN, Wu G, Hogenesch JB, Sehgal A. 2016. Neural clocks and Neuropeptide F/Y regulate circadian gene expression in a peripheral metabolic tissue. eLife **5**:e13552. DOI: https://doi.org/10.7554/eLife.13552

Franco DL, Frenkel L, Ceriani MF. 2018. The Underlying Genetics of *Drosophila* Circadian Behaviors. Physiology **33**:50–62. DOI: https://doi.org/10.1152/physiol.00020.2017, PMID: 29212892

Fujii S, Toyama A, Amrein H. 2008. A male-specific fatty acid omega-hydroxylase, SXE1, is necessary for efficient male mating in Drosophila melanogaster. Genetics **180**:179–190. DOI: https://doi.org/10.1534/genetics.108.089177, PMID: 18716335

Grima B, Chélot E, Xia R, Rouyer F. 2004. Morning and evening peaks of activity rely on different clock neurons of the Drosophila brain. Nature **431**:869–873. DOI: https://doi.org/10.1038/nature02935

Gummadova JO, Coutts GA, Glossop NRJ. 2009. Analysis of the Drosophila Clock promoter reveals heterogeneity in expression between subgroups of central oscillator cells and identifies a novel enhancer region. Journal of biological rhythms **24**:353–367. DOI: https://doi.org/10.1177/0748730409343890, PMID: 19755581

Guo F, Chen X, Rosbash M. 2017. Temporal calcium profiling of specific circadian neurons in freely moving flies. Proceedings of the National Academy of Sciences of the United States of America **114**:E8780–E8787. DOI: https://doi.org/10.1073/pnas.1706608114, PMID: 28973886

Guo F, Yu J, Jung HJ, Abruzzi KC, Luo W, Griffith LC, Rosbash M. 2016. Circadian neuron feedback controls the Drosophila sleep-activity profile. Nature **536**:292–297. DOI: https://doi.org/10.1038/nature19097

Hardin PE. 2005. The Circadian Timekeeping System of Drosophila. Current Biology **15**:R714–R722. DOI: https://doi.org/https://doi.org/10.1016/j.cub.2005.08.019

Helfrich-Förster C. 2005a. Neurobiology of the fruit fly's circadian clock. Genes, Brain and Behavior **4**:65–76. DOI: https://doi.org/10.1111/j.1601-183X.2004.00092.x

Helfrich-Förster C. 2005b. Neurobiology of the fruit fly's circadian clock. Genes, Brain and Behavior **4**:65–76. DOI: https://doi.org/10.1111/j.1601-183X.2004.00092.x

Helfrich-Förster C, Yoshii T, Wülbeck C, Grieshaber E, Rieger D, Bachleitner W, Cusumano P, Rouyer F. 2007. The lateral and dorsal neurons of Drosophila melanogaster: New insights about their morphology and function. Cold Spring Harbor Symposia on Quantitative Biology **72**:517–525. DOI: https://doi.org/10.1101/sqb.2007.72.063, PMID: 18419311

Hermann-Luibl C, Helfrich-Förster C. 2015. Clock network in Drosophila. Current opinion in insect science **7**:65–70. DOI: https://doi.org/10.1016/j.cois.2014.11.003, PMID: 32846682

Herrero A, Duhart JM, Ceriani MF. 2017. Neuronal and glial clocks underlying structural remodeling of pacemaker neurons in Drosophila. Frontiers in Physiology **8**:1–10. DOI: https://doi.org/10.3389/fphys.2017.00918

Howlader G, Paranjpe DA, Sharma VK. 2006a. Non-ventral lateral neuron-based, non-PDF-mediated clocks control circadian egg-laying rhythm in Drosophila melanogaster. Journal of Biological Rhythms **21**:13–20. DOI: https://doi.org/10.1177/0748730405282882, PMID: 16461981

Howlader G, Paranjpe DA, Sharma VK. 2006b. Non-ventral lateral neuron-based, non-PDF-mediated clocks control circadian egg-laying rhythm in Drosophila melanogaster. Journal of Biological Rhythms **21**:13–20. DOI: https://doi.org/10.1177/0748730405282882, PMID: 16461981

Howlader G, Sharma VK. 2006. Circadian regulation of egg-laying behavior in fruit flies Drosophila melanogaster. Journal of Insect Physiology **52**:779–785. DOI: https://doi.org/10.1016/j.jinsphys.2006.05.001, PMID: 16781727

Im SH, Li W, Taghert PH. 2011. PDFR and CRY signaling converge in a subset of clock neurons to modulate the amplitude and phase of circadian behavior in Drosophila. PloS one **6**:e18974. DOI: https://doi.org/10.1371/journal.pone.0018974, PMID: 21559487

Ito C, Tomioka K. 2016. Heterogeneity of the peripheral circadian systems in Drosophila melanogaster: A review. Frontiers in Physiology **7**:1–7. DOI: https://doi.org/10.3389/fphys.2016.00008, PMID: 26858652

Kaufman BP, Demerec M. 1942. Utilization of Sperm by the Female Drosophila Melanogaster. The American Naturalist **76**:445–469.

Konopka RJ, Benzer S. 1971. Clock mutants of Drosophila melanogaster. Proceedings of the National Academy of Sciences of the United States of America **68**:2112–6. DOI: https://doi.org/10.1073/pnas.68.9.2112, PMID: 5002428

Li J, Ning C, Liu Y, Deng B, Wang B, Shi K, Wang R, Fang R, Zhou C. 2023. Prothoracicotropic hormone controls female sexual receptivity through the function of ecdysone in pC1 neurons of*Drosophila*. DOI: https://doi.org/10.1101/2023.09.28.559939

Ma D, Przybylski D, Abruzzi KC, Schlichting M, Li Q, Long X, Rosbash M. 2021. A transcriptomic taxonomy of drosophila circadian neurons around the clock. eLife **10**:1–19. DOI: https://doi.org/10.7554/eLife.63056, PMID: 33438579

Manjunatha T, Hari Dass S, Sharma VK. 2008. Egg-laying rhythm in Drosophila melanogaster. Journal of Genetics **87**:495–504. DOI: https://doi.org/10.1007/s12041-008-0072-9, PMID: 19147938

McCabe C, Birley A. 1998a. Oviposition in the period genotypes of Drosophila melanogaster. Chronobiology International **15**:119–133. DOI: https://doi.org/10.3109/07420529808998677, PMID: 9562917

McCabe C, Birley A. 1998b. Oviposition in the period genotypes of Drosophila melanogaster. Chronobiology International **15**:119–133. DOI: https://doi.org/10.3109/07420529808998677, PMID: 9562917

Menon A, Varma V, Sharma VK. 2014a. Rhythmic egg-laying behaviour in virgin females of fruit flies Drosophila melanogaster. Chronobiology International **31**:433–441. DOI: https://doi.org/10.3109/07420528.2013.866131, PMID: 24328816

Menon A, Varma V, Sharma VK. 2014b. Rhythmic egg-laying behaviour in virgin females of fruit flies Drosophila melanogaster. Chronobiology International **31**:433–441. DOI: https://doi.org/10.3109/07420528.2013.866131, PMID: 24328816

Myers EM, Yu J, Sehgal A. 2003. Circadian Control of Eclosion: Interaction between a Central and Peripheral Clock in Drosophila melanogaster. Current Biology **13**:526–533. DOI: https://doi.org/10.1016/S0960-9822(03)00167-2

Pfeiffenberger C, Lear BC, Keegan KP, Allada R. 2010. Processing sleep data created with the Drosophila activity monitoring (DAM) system. Cold Spring Harbor Protocols **5**:1251–1257. DOI: https://doi.org/10.1101/pdb.prot5520

Picot M, Cusumano P, Klarsfeld A, Ueda R, Rouyer F. 2007. Light Activates Output from Evening Neurons and Inhibits Output from Morning Neurons in the Drosophila Circadian Clock. PLOS Biology **5**:e315.

Reinhard N, Bertolini E, Saito A, Sekiguchi M, Yoshii T, Rieger D, Helfrich-Förster C. 2022. The lateral posterior clock neurons of Drosophila melanogaster express three neuropeptides and have multiple connections within the circadian clock network and beyond. The Journal of comparative neurology **530**:1507–1529. DOI: https://doi.org/10.1002/cne.25294, PMID: 34961936

Reinhard N, Fukuda A, Manoli G, Derksen E, Saito A, Möller G, Sekiguchi M, Rieger D, Helfrich-Förster C, Yoshii T, Zandawala M. 2024. Synaptic connectome of the Drosophila circadian clock. Nature Communications **15**. DOI: https://doi.org/10.1038/s41467-024-54694-0, PMID: 39638801

Renn SCP, Park JH, Rosbash M, Hall JC, Taghert PH. 1999. A pdf neuropeptide gene mutation and ablation of PDF neurons each cause severe abnormalities of behavioral circadian rhythms in Drosophila. Cell **99**:791–802. DOI: https://doi.org/10.1016/S0092-8674(00)81676-1, PMID: 10619432

Richardson JTE. 2011. The analysis of 2 × 2 contingency tables-Yet again. *Statistics in Medicine*. DOI: https://doi.org/10.1002/sim.4116, PMID: 21432882

Riva S, Ispizua JI, Breide MT, Polcowñuk S, Lobera JR, Ceriani MF, Risau-Gusman S, Franco DL. 2022. Mating disrupts morning anticipation in Drosophila melanogaster females. PLoS Genetics **18**:1–20. DOI: https://doi.org/10.1371/journal.pgen.1010258, PMID: 36548223

Ruf T. 1999. The Lomb-Scargle Periodogram in Biological Rhythm Research: Analysis of Incomplete and Unequally Spaced Time-Series. Biological Rhythm Research **30**:178–201. DOI: https://doi.org/10.1076/brhm.30.2.178.1422

Sakai T, Ishida N. 2001. Circadian rhythms of female mating activity governed by clock genes in Drosophila. Proceedings of the National Academy of Sciences **98**:9221–9225. DOI: https://doi.org/10.1073/pnas.151443298

Scheffer LK, Xu CS, Januszewski M, Lu Z, Takemura SY, Hayworth KJ, Huang GB, Shinomiya K, Maitin-Shepard J, Berg S, Clements J, Hubbard PM, Katz WT, Umayam L, Zhao T, Ackerman D, Blakely T, Bogovic J, Dolafi T, Kainmueller D, Kawase T, Khairy KA, Leavitt L, Li PH, Lindsey L, Neubarth N, Olbris DJ, Otsuna H, Trautman ET, Ito M, Bates AS, Goldammer J, Wolff T, Svirskas R, Schlegel P, Neace ER, Knecht CJ, Alvarado CX, Bailey DA, Ballinger S, Borycz JA, Canino BS, Cheatham N, Cook M, Dreher M, Duclos O, Eubanks B, Fairbanks K, Finley S, Forknall N, Francis A, Hopkins GP, Joyce EM, Kim S, Kirk NA, Kovalyak J, Lauchie SA, Lohff A, Maldonado C, Manley EA, McLin S, Mooney C, Ndama M, Ogundeyi O, Okeoma N, Ordish C, Padilla N, Patrick C, Paterson T, Phillips EE, Phillips EM, Rampally N, Ribeiro C, Robertson MK, Rymer JT, Ryan SM, Sammons M, Scott AK, Scott AL, Shinomiya A, Smith C, Smith K, Smith NL, Sobeski MA, Suleiman A, Swift J, Takemura S, Talebi I, Tarnogorska D, Tenshaw E, Tokhi T, Walsh JJ, Yang T, Horne JA, Li F, Parekh R, Rivlin PK, Jayaraman V, Costa M, Jefferis GSXE, Ito K, Saalfeld S, George R, Meinertzhagen

IA, Rubin GM, Hess HF, Jain V, Plaza SM. 2020. A connectome and analysis of the adult drosophila central brain. eLife **9**:1–74. DOI: https://doi.org/10.7554/ELIFE.57443, PMID: 32880371

Schlichting M, Díaz MM, Xin J, Rosbash M. 2019. Neuron-specific knockouts indicate the importance of network communication to drosophila rhythmicity. eLife **8**:1–20. DOI: https://doi.org/10.7554/eLife.48301, PMID: 31613223

Shafer OT, Gutierrez GJ, Li K, Mildenhall A, Spira D, Marty J, Lazar AA, Fernandez MP. 2022. Connectomic Analysis of the Drosophila Lateral Neuron Clock Cells Reveals the Synaptic Basis of Functional Pacemaker Classes. eLife **11**:1–29. DOI: https://doi.org/10.7554/eLife.79139, PMID: 35766361

Shannon P, Markiel A, Ozier O, Baliga NS, Wang JT, Ramage D, Amin N, Schwikowski B, Ideker T. 2003. Cytoscape: a software environment for integrated models of biomolecular interaction networks. Genome research **13**:2498–2504. DOI: https://doi.org/10.1101/gr.1239303, PMID: 14597658

Sheeba V, Chandrashekaran MK, Joshi A, Sharma VK. 2001a. Persistence of oviposition rhythm in individuals of Drosophila melanogaster reared in an aperiodic environment for several hundred generations. Journal of Experimental Zoology **290**:541–549. DOI: https://doi.org/https://doi.org/10.1002/jez.1098

Sheeba V, Chandrashekaran MK, Joshi A, Sharma VK. 2001b. Persistence of oviposition rhythm in individuals of Drosophila melanogaster reared in an aperiodic environment for several hundred generations. Journal of Experimental Zoology **290**:541–549. DOI: https://doi.org/https://doi.org/10.1002/jez.1098

Shindey R, Varma V, Nikhil KL, Sharma VK. 2017. Evolution of circadian rhythms in Drosophila melanogaster populations reared in constant light and dark regimes for over 330 generations. Chronobiology International **34**:537–550. DOI: https://doi.org/10.1080/07420528.2016.1195397, PMID: 28156168

Stoleru D, Peng Y, Agosto J, Rosbash M. 2004. Coupled oscillators control morning and evening locomotor behaviour of Drosophila. Nature **431**:862–868. DOI: https://doi.org/10.1038/nature02926

Tanoue S, Krishnan P, Krishnan B, Dryer SE, Hardin PE. 2004. Circadian Clocks in Antennal Neurons Are Necessary and Sufficient for Olfaction Rhythms in Drosophila. Current Biology **14**:638–649. DOI: https://doi.org/10.1016/j.cub.2004.04.009

Tataroglu O, Emery P. 2015. The molecular ticks of the Drosophila circadian clock. Current Opinion in Insect Science **7**:51–57. DOI: https://doi.org/10.1016/j.cois.2015.01.002

van Drongelen W. 2007. Signal processing for neuroscientists: Introduction to the analysis of physiological signals.

VanderPlas JT. 2018. Understanding the Lomb–Scargle Periodogram. The Astrophysical Journal Supplement Series **236**:16. DOI: https://doi.org/10.3847/1538-4365/aab766

Vijayan V, Wang F, Wang K, Chakravorty A, Adachi A, Akhlaghpour H, Dickson BJ, Maimon G. 2023a. A rise-to-threshold process for a relative-value decision. Nature **619**:563–571. DOI: https://doi.org/10.1038/s41586-023-06271-6, PMID: 37407812

Vijayan V, Wang F, Wang K, Chakravorty A, Adachi A, Akhlaghpour H, Dickson BJ, Maimon G. 2023b. A rise-to-threshold process for a relative-value decision. Nature **619**:563–571. DOI: https://doi.org/10.1038/s41586-023-06271-6, PMID: 37407812

Wang F, Wang K, Forknall N, Patrick C, Yang T, Parekh R, Bock D, Dickson BJ. 2020. Neural circuitry linking mating and egg laying in Drosophila females. Nature **579**:101–105. DOI: https://doi.org/10.1038/s41586-020-2055-9

Yang C, Belawat P, Hafen E, Jan LY, Jan Y. 2008. Drosophila Egg-Laying Site Selection as a Systen to Study Simple Decision-Making Processes. 1679–1684.

Yoshii T, Rieger D, Förster CH. 2012. Two clocks in the brain: An update of the morning and evening oscillator model in Drosophila. Progress in Brain Research **199**:59–82. DOI: https://doi.org/10.1016/B978-0-444-59427-3.00027-7, PMID: 22877659

Yoshii T, Todo T, Wülbeck C, Stanewsky R, Helfrich-Förster C. 2008. Cryptochrome is present in the compound eyes and a subset of Drosophila's clock neurons. The Journal of comparative neurology **508**:952–966. DOI: https://doi.org/10.1002/cne.21702, PMID: 18399544

Yoshii T, Wulbeck C, Sehadova H, Veleri S, Bichler D, Stanewsky R, Helfrich-Forster C, Wülbeck C, Sehadova H, Veleri S, Bichler D, Stanewsky R, Helfrich-Förster C. 2009. The neuropeptide pigment-dispersing factor adjusts period and phase of Drosophila's clock. Journal of Neuroscience **29**:2597–2610. DOI: https://doi.org/10.1523/JNEUROSCI.5439-08.2009, PMID: 19244536

Zhang C, Daubnerova I, Jang YH, Kondo S, Žitnan D, Kim YJ. 2021. The neuropeptide allatostatin C from clock-associated DN1p neurons generates the circadian rhythm for oogenesis. Proceedings of the National Academy of Sciences of the United States of America **118**. DOI: https://doi.org/10.1073/pnas.2016878118, PMID: 33479181

Zhang Y, Liu Y, Bilodeau-Wentworth D, Hardin PE, Emery P. 2010. Light and Temperature Control the Contribution of Specific DN1 Neurons to Drosophila Circadian Behavior. Current Biology **20**:600–605. DOI: https://doi.org/10.1016/j.cub.2010.02.044

Zhou C, Pan Y, Robinett CC, Meissner GW, Baker BS. 2014. Central brain neurons expressing doublesex regulate female receptivity in Drosophila. Neuron **83**:149–163. DOI: https://doi.org/10.1016/j.neuron.2014.05.038, PMID: 24991959

ACKNOWLEDGEMENTS

This work was supported by the Agencia Nacional de Promoción Científica y Tecnológica (Grants PICT-2016-1042 to S.R.G; PICT PICT2019-1015 to MFC and PICT-2021-00213 to D.L.F.), the Universidad Nacional del Comahue, CRUB (Grant 04/B239 to D.L.F.). D.L.F., S.R.G and M.F.C. are members of the Argentine Research Council for Science and Technology (CONICET). SR holds a graduate fellowship from CONICET. Stocks obtained from the Bloomington Drosophila Stock Center (NIH P40OD018537), were used in this study. We thank Lucas Mongiat for helpful discussions and critical reading of the manuscript.

AUTHOR CONTRIBUTIONS

Conceptualization, Methodology and Validation: S.R; S.R.G; D.L.F; Formal Analysis, Investigation, and Visualization, S.R; S.R.G; D.L.F; Writing – Original Draft, S.R; S.R.G; D.L.F; Writing – Review & Editing: S.R, M.F.C; S.R.G, D.L.F ; Supervision, S.R.G, D.L.F ; Project Administration and Funding Acquisition, M.F.C, S.R.G., D.L.F.

DECLARATION OF INTEREST

The authors declare no competing financial interests.

DATA AVAILABILITY

All data are available in the following links:

https://github.com/srisaug/flywork/blob/main/RawData_Rivaetal_eLife2025_Fig4_+>UAS-perRNAi.zip

https://github.com/srisaug/flywork/blob/main/RawData_Rivaetal_eLife2025_Fig4_MB122Bsplit-Gal4>+.zip

https://github.com/srisaug/flywork/blob/main/RawData_Rivaetal_eLife2025_Fig4_MB122Bsplit-Gal4>UAS-perRNAi.zip

https://github.com/srisaug/flywork/blob/main/RawData_Rivaetal_eLife2025_Figures123.zip

Supplementary material for:

Circadian control of a sex-specific behaviour in Drosophila

Sabrina Riva[1], M. Fernanda Ceriani[2], Sebastián Risau-Gusman[1,*], D. Lorena Franco[1,*]

1. Medical Physics Department, Bariloche Atomic Center, Comisión Nacional de Energía Atómica (CNEA) and Consejo Nacional de Investigaciones Científicas y Técnicas (CONICET), San Carlos de Bariloche, Argentina;

2. Laboratorio de Genética del Comportamiento. Fundación Instituto Leloir - IIBBA - CONICET, Buenos Aires, C1405BWE, Argentina.

∗ Corresponding authors; e-mail: lorena.franco@cab.cnea.gov.ar; srisau@cab.cnea.gov.ar.

Contents

S1 Supplementary figures to the main text **2**

S2 Supplementary Table 1 **12**

S3 Method used for the assessment of rhythmicity **13**

S1 Supplementary figures to the main text

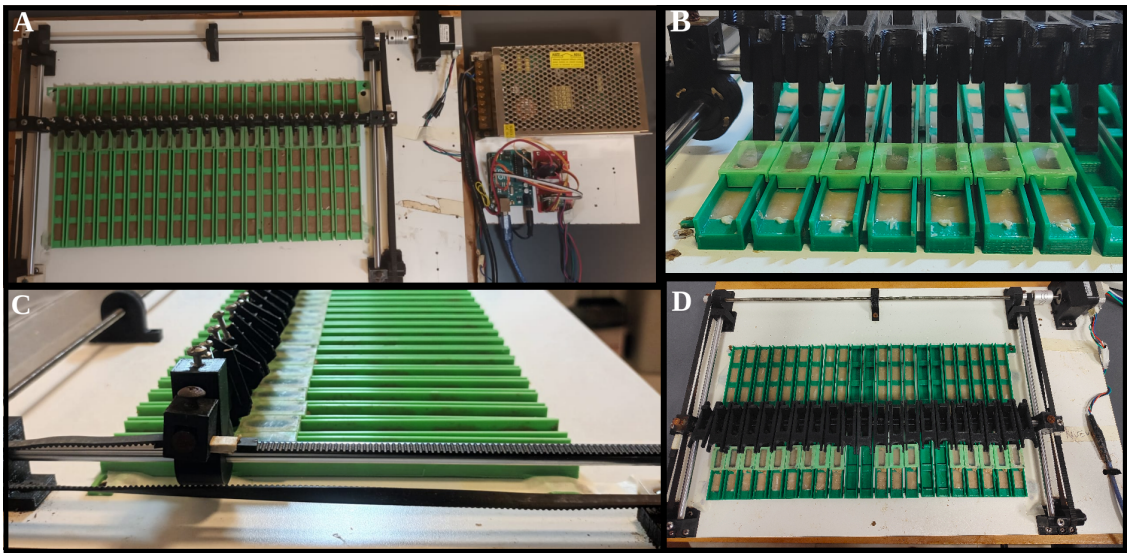

Figure 1S1: **Semi-automated egg collection device.** **A**: View from above. The white square is the wooden base to which there are two bars attached that hold the mechanical arm (in black), moved by a stepper motor (black box in the upper right corner of the wooden base). The arm shifts forward (downward in the picture) each fly chamber (light green box) from one well to the next. **B**: Detail of the tracks (dark green) holding the fly chambers, and the food wells filled with banana medium (brown) and a drop of yeast (white). **C**: Lateral view of the tracks. **D**: Detail from above, showing the plastic piece used to press the chambers against the tracks.

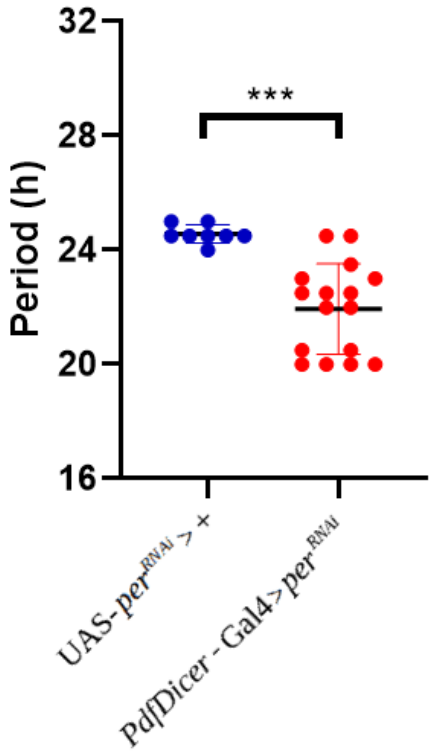

Figure 2S1: **Disruption of the molecular clock in PDF+ neurons causes a shortening of the egg-laying period at the individual level.** Period of egg-laying rhythms for rhythmic individual flies (UAS-per^{RNAi}, n=8 (out of 18), *PdfDicer*-Gal4>UAS-per^{RNAi}, n=16 (out of 34). ***: $p < 0.001$ (chi-squared test).

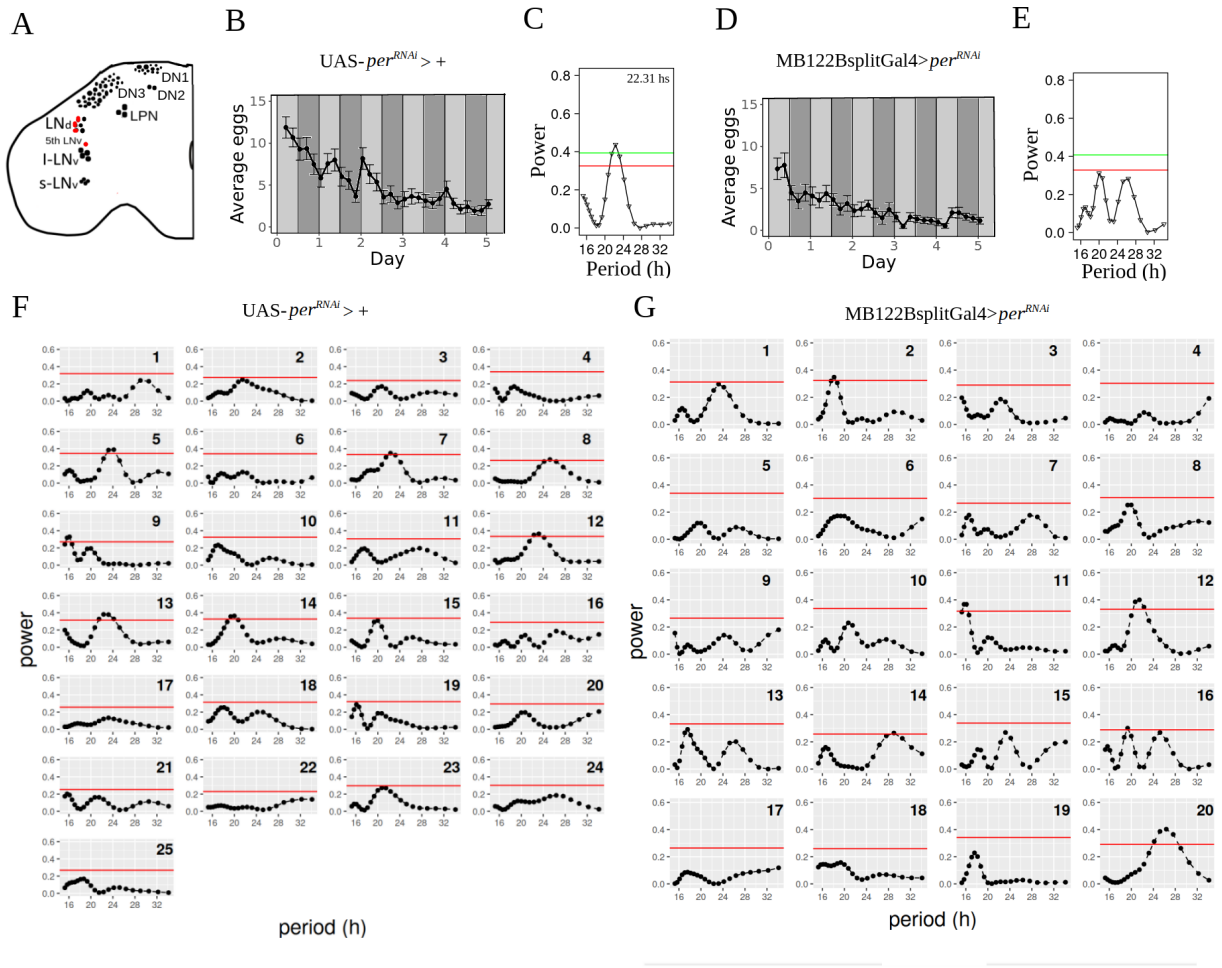

Figure 3S1: **Disruption of the molecular clock in Cry+ LNd neurons drastically reduces the circadian rhythmicity of oviposition.** **A**: Schematic diagram of the neurons (painted in red) where the molecular clocks have been disrupted. **B, D**: Average eggs collected as a function of time. The average was made with all flies (Strongly rhythmic, weakly rhythmic and arrhythmic). White and dark gray bars represent periods of lights on and off respectively (LD), whereas light gray bars represent subjective days in DD, (i.e times where lights were on at rearing, but are now off). **C, E**: Periodograms of the average time series of the number of eggs laid by all females. **F, G**: Periodograms of the individual time series of the number of eggs laid. Red and green horizontal lines represent significances of 0.05 and 0.01, respectively. **B, C, F**: control (+>UAS-per^{RNAi}, n=25). **D, E, G**: MB122BsplitGal4>per^{RNAi} (MB122B-splitGal4>UAS-per^{RNAi}, n=20).

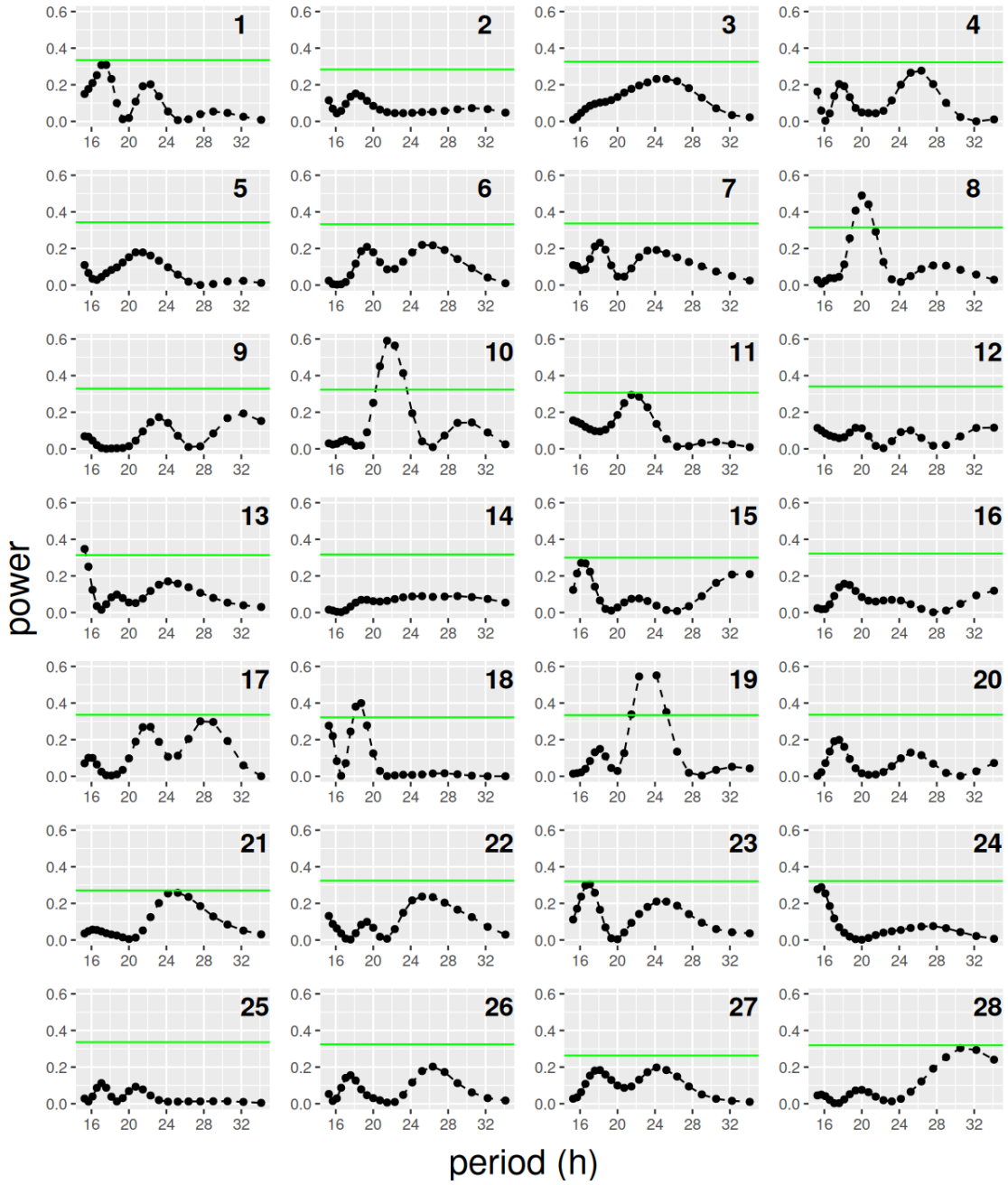

Figure 3S2: **Individual periodograms for the records obtained after applying detrending for the experiment in DD with Mai179-Gal4;pdf-Gal80 >UAS-per^{RNAi} (n=28) female flies described in the main text.** Green horizontal lines represent significances of p=0.05.

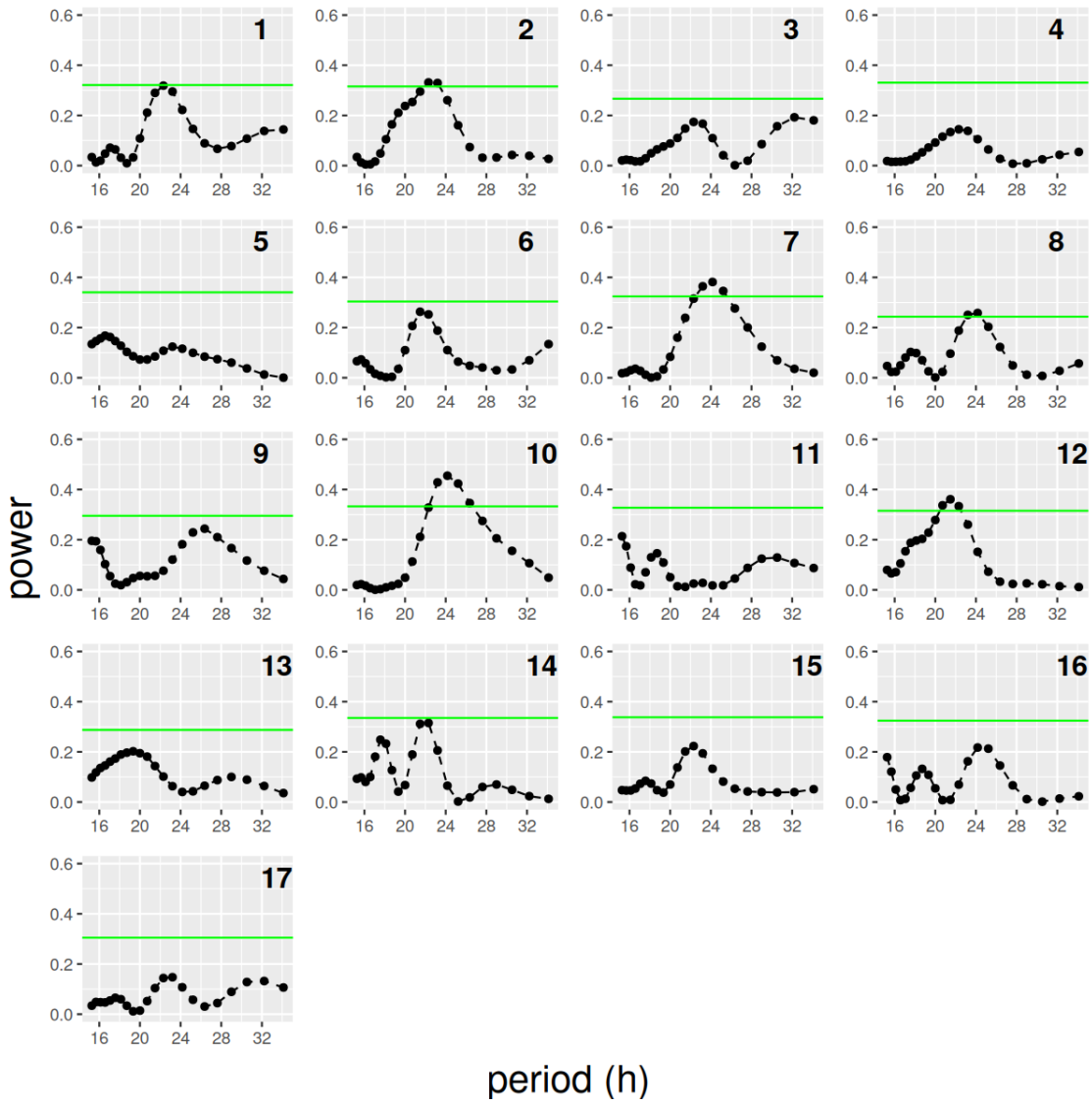

Figure 3S3: **Individual periodograms for the records obtained after applying detrending for the experiment in DD with Mai179-Gal4;pdf-Gal80>+ (n=17) female flies described in the main text.** Green horizontal lines represent significances of p=0.05.

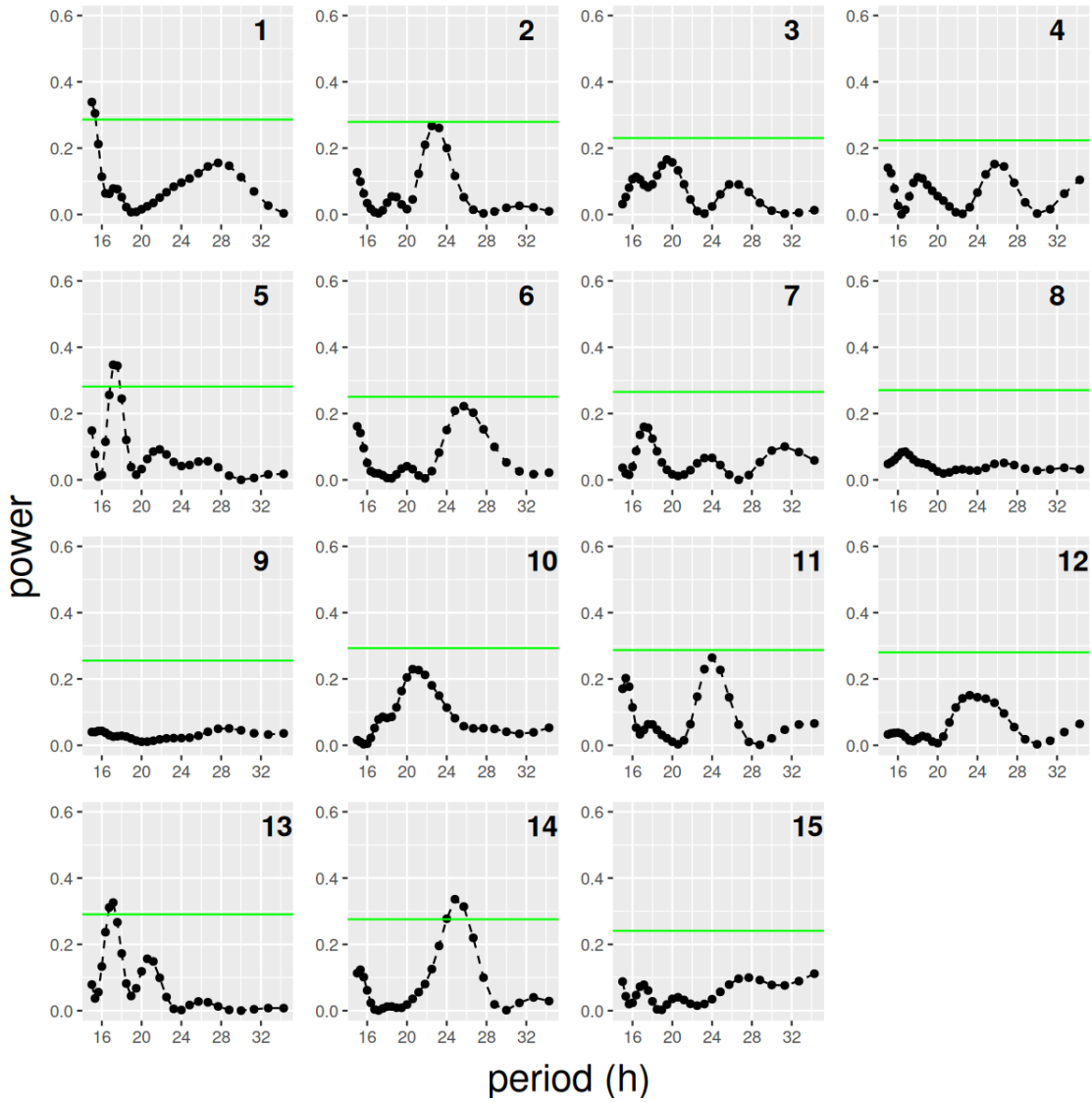

Figure 3S4: **Individual periodograms for the records obtained after applying detrending for the experiment in DD with +>UAS-per^{RNAi}, (n=15) female flies described in the main text.** Green horizontal lines represent significances of p=0.05.

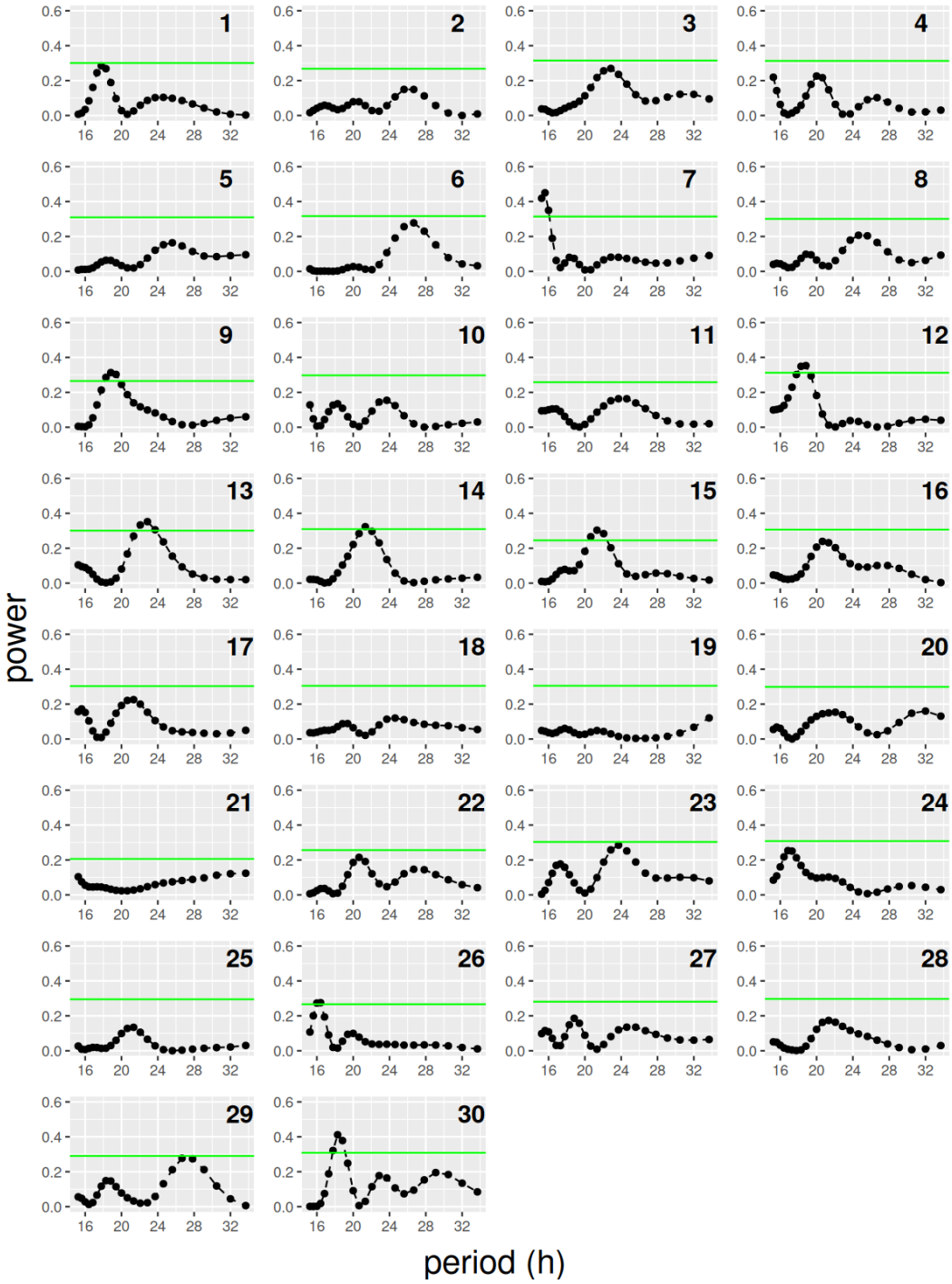

Figure 3S5: **Individual periodograms for the records obtained after applying detrending for the experiment in DD MB122Bsplit-Gal4>UAS-cyc^{DN} (n=30) female flies described in the main text.** Green horizontal lines represent significances of p=0.05.

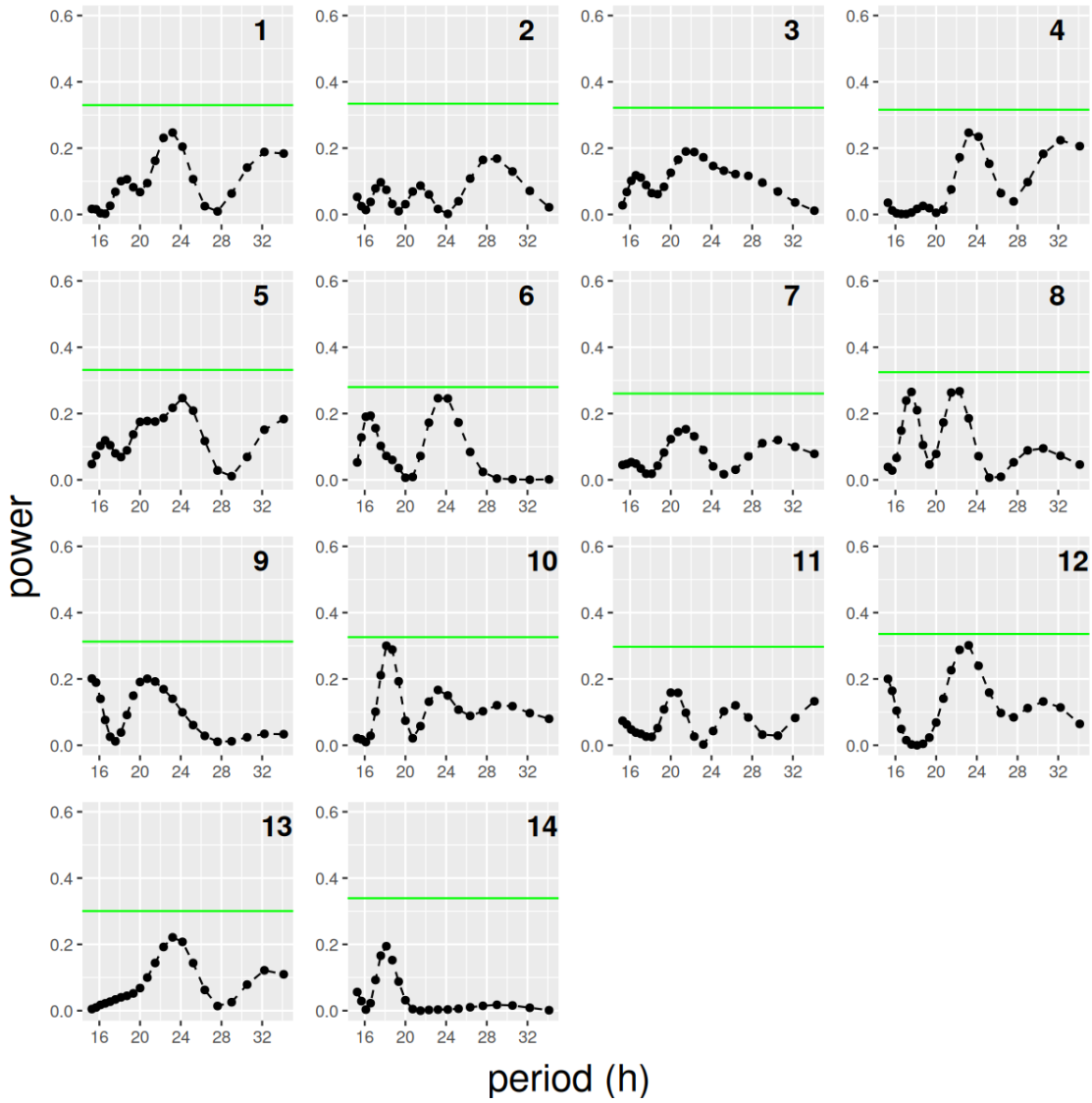

Figure 3S6: **Individual periodograms for the records obtained after applying detrending for the experiment in DD with MB122Bsplit-Gal4>+ (n=14) female flies described in the main text.** Green horizontal lines represent significances of p=0.05.

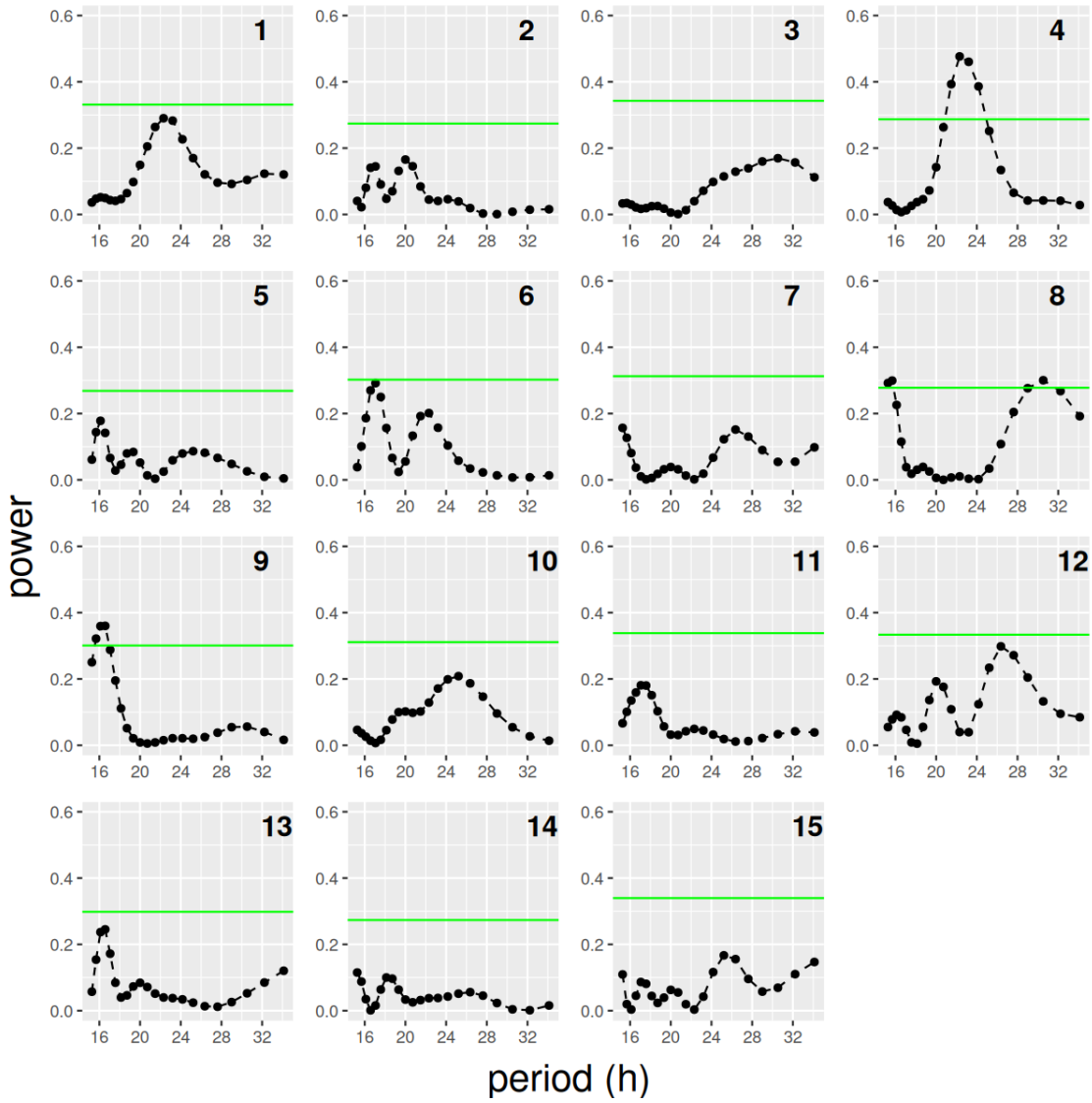

Figure 3S7: **Individual periodograms for the records obtained after applying detrending for the experiment in DD with +>UAS-cyc^{DN} (n=15) female flies described in the main text.** Green horizontal lines represent significances of p=0.05.

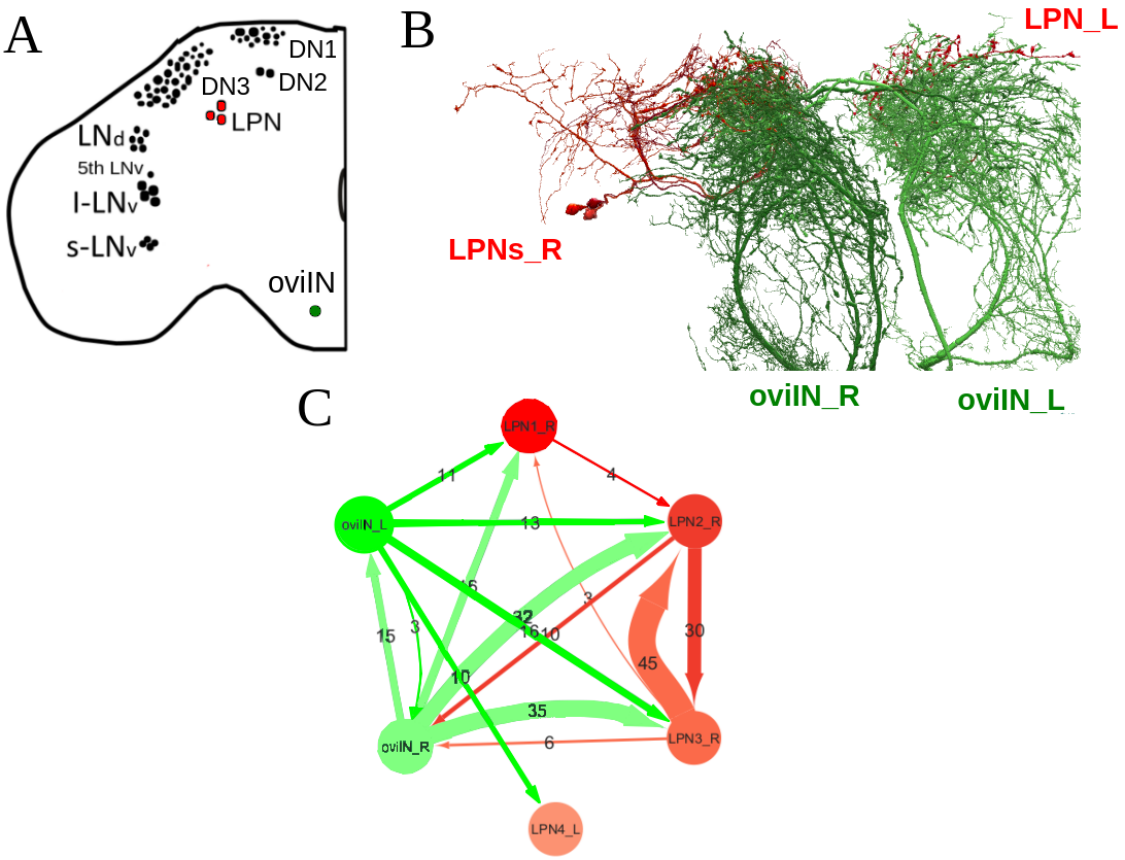

Figure 5S1: **Direct synaptic connections between LPN and oviposition-related neurons in the hemibrain dataset.** **A**: Scheme showing the neurons analyzed (in color). **B**: Connection between LPN and oviIN neurons. **C**: Network representation of the connectivity between these neurons. Numbers give the number of synaptic contacts, which represent the strength of the connections. Only intermediate (between 3 and 9 synaptic contacts) and strong ($>$ 9 synaptic contacts) connections are considered

S2 Supplementary Table 1

Genotype	$\tau \pm$ sd	R	n
+>UAS-per^{RNAi}	23.8 $\pm$ 0.1	87.5 $(21/24)^a$	24
Clk856-Gal4>+	23.8 $\pm$ 0.1	96.15 $(25/26)^a$	26
Clk856-Gal4>UAS-per^{RNAi}	25.9 $\pm$ 0.3	38.09 $(8/21)^b$	21

Table S1: **Downregulation of *per* in all clock brain neurons impairs locomotor circadian activity:** Analysis of the period (τ) and percentage of rhythmicity (R) between genotypes. Different letters indicate statistically significant differences ($p < 0.05$, One-way ANOVA with a Tukey post-hoc test). n indicates the number of animals tested.

S3 Method used for the assessment of rhythmicity

The egg records of single, isolated, female fruit flies display several distinct features that complicate the assessment of rhythmicity. The recorded variable is discrete and typically takes only a few values, which depend on how often it is sampled. The more often is is sampled, the less number of values the variable takes. Thus, it is only possible to sample it a few times (usually less than ten) per cycle. As shown below, for noisy signals this feature tends to make the assessment of rhythmicity much more complicated, compared with signals with the same levels of noise, but that are sampled more often (as happens with activity records).

The particularities of egg-laying in Drosophila add further complications. First, the number of eggs laid has a clearly descending trend (probably due to the depletion of the sperm stored in the female spermatheque). Second, this behavior seems to be particularly "noisy", in the sense that the decision of laying an egg seems to depend not only on the time of the day, but also on many other stimuli. As a consequence, any method that tries to assess the presence of a rhythm must be able to subtract, at least partially, the effects of trend and noise. In the following we describe the method we have used to achieve this aim.

Noise effects and subtraction

We use Lomb-Scargle (LS) periodograms (Ruf (1999); Zielinski et al. (2014)) to determine if a signal is rhythmic, and to estimate its period. It is important to note that, as happens with Discrete Fourier Transforms, periodograms only give information about a number of predetermined periods (usually called the "frequency grid"), and the number of available periods (and therefore the resolution with which the true period of the signal can be ascertained) is proportional to the time length of the signal. The significance lines are obtained by repeatedly shuffling the signal and recording the highest peaks of the resulting periodograms. Thus, a $p = 0.05$ significance line at a given power means that in 95% of the shufflings the highest peak was below the line.

In order to understand the effect on the assessment of rhythmicity of having few observations

per cycle, we have generated noisy harmonic signals and, for the same signal, we have taken different numbers of "observations" (i.e. we have sampled the signals with different rates), and we have compared the results of period determination in each case. For a signal with period $T = 24$ with Gaussian noise added, panels A and C of Fig. S1 show an example of observations made every 30 minutes (A), which corresponds to a sampling rate usual in activity records (Pfeiffenberger et al. (2010)) or every 4 hours (B), more typical of oviposition records. Even though in the corresponding LS periodograms (panels B and D, respectively) the highest peak is at $T = 24h$, the power of this peak (p_p) is smaller than the power p_σ corresponding to a significance of $\sigma = 0.05$ (i.e. the peak is not significant) when the number of observations is small, whereas it is much bigger that p_σ when the number of observations is larger. Repeating this experiment for different numbers of observations (panel E), confirms that, on average, sampling a signal less often (i.e. taking less observations per cycle) strongly decreases the significance of the peaks obtained.

Since oviposition records have few observations per cycle, we have resorted to the method of taking population averages (Semmlow (2018)), in order to get rid of some of the noise. This implies assuming that the underlying periodic signal is basically the same for all individuals, in terms of period and phase. This seems to be a reasonable assumption since activity records consistently show that, after lights off the periods of activity and sleep tend to be synchronized, at least during the first days.

Trend subtraction

When a continuous signal is considered as the product $h(t) = f(t)g(t)$ of a periodic signal $f(t)$ with a known period T, and a trend $g(t)$ that has little variation over a cycle, the classical method to uncouple them involves using moving averages (see, e.g. Hyndman (2021)):

$$g^*(t) = \frac{1}{T}\int_{t-T/2}^{t+T/2} h(t')dt'$$

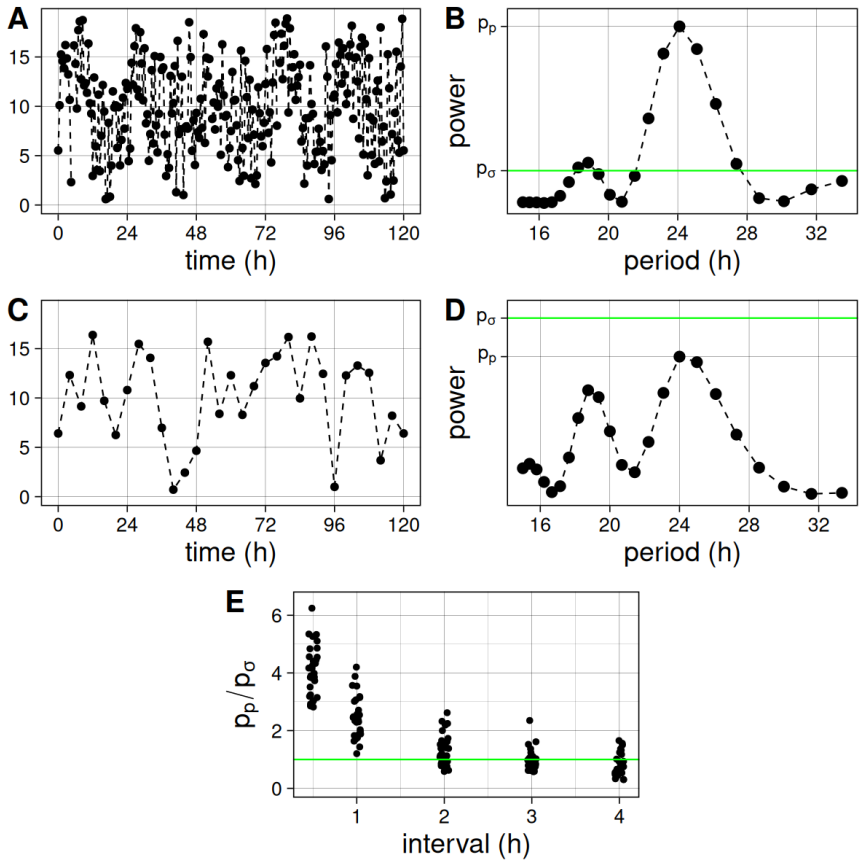

Figure S1: **Effect of noise in the assessment of rhythmicity of periodic signals.** **A,C**: Periodic signal with Gaussian noise (average=0, sd=2), sampled at intervals of 30 minutes (A) or 4 hours (C). **B,D**: Periodograms of the signals shown in panel A and C, respectively. **E**: Comparison of periodogram peak heights (relative to the significance level) for 150 signals sampled at different intervals. p_p is the power of the periodogram peak, whereas p_σ denotes the power corresponding to a significance level $\sigma = 0.05$. The green line, corresponding to $p_s = p_\sigma$, separates experiments where the peaks are significant (above) from those where peaks are not significant (below).

$$f^*(t) \quad = \quad h(t)/g^*(t) \tag{S1}$$

where $g^*(t)$ and $f^*(t)$ are the estimates of the trend and the periodic signal. When the assumptions mentioned are met, the estimates coincide with the original functions.

In our case, however, many things are different. The most important are that we do not

know what is the period of the "periodic" signal (in fact, we want an estimate of T if the signal is periodic at all), and that the signal is not continuous. The first feature implies that we ignore what is the "correct" value for the size for the moving average. The second feature forces us to convert the moving average integral into a sum with few terms. As a consequence, for a time series of the form $f(0), f(4), f(8), ...$, representing observations on the number of eggs taken every 4 hours, we use the following equations for estimating the trend and the underlying periodic signal:

$$\begin{aligned} g^*(t_i) &= \frac{1}{2n+1} \sum_{j=i-n}^{i+n} h(t_j) \\ f^*(t_i) &= h(t_i)/g^*(t_i) \end{aligned} \tag{S2}$$

where t_i is the time at which the i-th observation was made. We have used $n = 3$, corresponding to a moving average of roughly 28 hours (using $n = 2$, i.e. 20 hours, gives very similar results).

In order to test our method we apply it here to "synthetic" egg records, generated with the following model. We assume that there is an underlying signal $f(t)$ of period T (time is measured in hours), given by

$$f(t) = A(1 + \sin(0.1 + 2\pi t/T), \tag{S3}$$

with $A = 20$ (maximum of eggs at each time point), and that this is corrupted by some additive noise $n(t)$. For simplicity, $n(t)$ is simply a random number uniformly chosen between 0 and A. The resulting signal is modulated by a decay given by $g(t) = \exp(-t/50)$. The total signal is then

$$h(t) = int[g(t)(\alpha f(t) + (1-\alpha)n(t))], t \in \{0, 4, 8, ..., 120\}. \tag{S4}$$

Fig. S2 shows a graphical example of the partial detrending of a synthetic signal. Panels A and B show, respectively, the synthetic decay and noisy rhyhmic signal, with period $T = 23.8$, which give the signal shown in panel D, when combined. Notice that when a periodogram of the signal in B is generated, the peak is close but not exactly in 23.8 h, simply because this frequency is not available in the frequency grid. The periodogram of the full signal (panel E) shows that the decay complicates the determination of rhythmicity, since the peak is now under the significance line. Panels F and G show our estimates for the decay and the noisy rhythmic signal obtained

with our method. The periodogram of the signal in G (panel H) confirms that it is rhythmic and with the same period as the original (panel B).

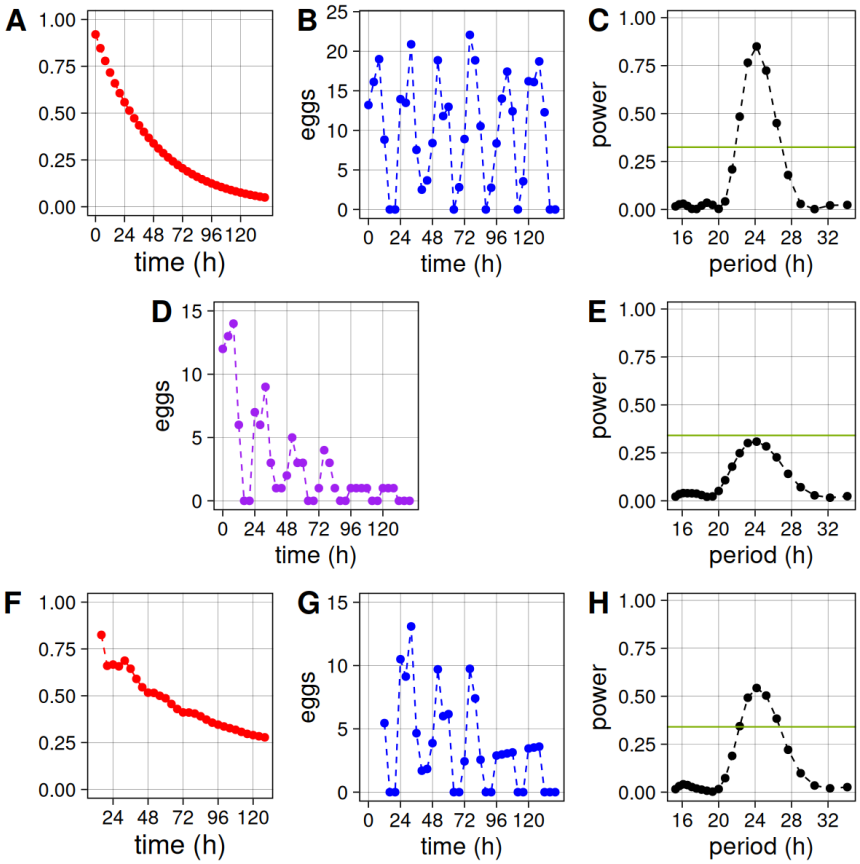

Figure S2: **Generation and decomposition of a decaying noisy rhythmic synthetic signal.** **A**: Modulating decay function. **B**: Noisy rhythmic signal. **D**: Signal given by the product of signals A and B. **F**: Estimate of the decay function. **G**: Estimate of the rhythmic signal. **C**, **E**, **H**: Periodogram analysis of the signals in B, D, G, respectively. Green horizontal lines mark the power corresponding to a significance level of 0.05. Dashed lines are only guides to the eye.

Even though the size of the moving average window is fixed, the method is effective for assessing rhyhthmicity for decaying signals of very different periods, as shown in Fig. S3. Furthermore, when the signal is not rhythmic, the method gives a non-rhythmic estimate (panel D of Fig. S3). In order to check the accuracy of method estimation we generated 2000 synthetic sig-

nals with T between 19 and 28 hours (Fig. S4). First, it must be noticed that, even before adding decay, the estimation of period is not perfect, because of noise and the small number of cycles analyzed (panel A). When decay is added, the peaks in the periodogram are usually under the line of significance. Furthermore, if we use the position of these peaks as estimates, they tend to be clearly biased to larger values (panel B). When our method is applied, the estimates obtained are reasonably good, and there is almost no bias (panel C).

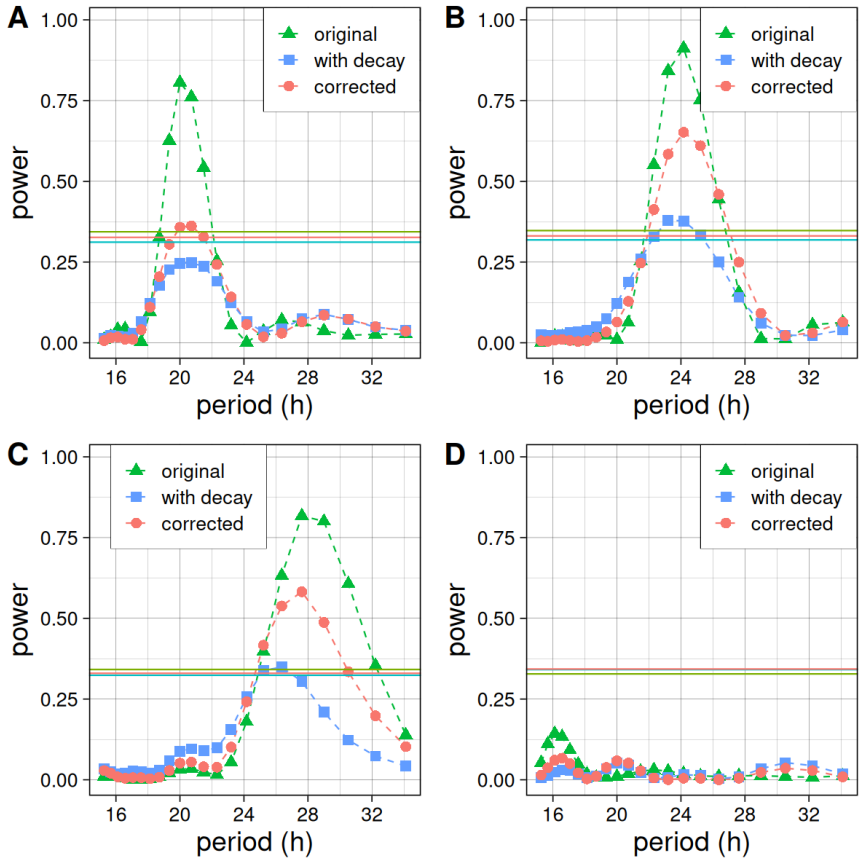

Figure S3: **Period determination for different synthetic signals.** Periodograms of rhythmic noisy signals with period T (green triangles), of the same signal with decay applied (blue squares), and of the estimation of the signal (red circles). **A**: $T = 20$. **B**: $T = 24$. **C**: $T = 28$. **D**: $\alpha = 0$ (i.e. purely arrhythmic signal). Each horizontal line corresponds to the significance level of 0.05 for the periodogram with matching color. Dashed lines are only guides to the eye.

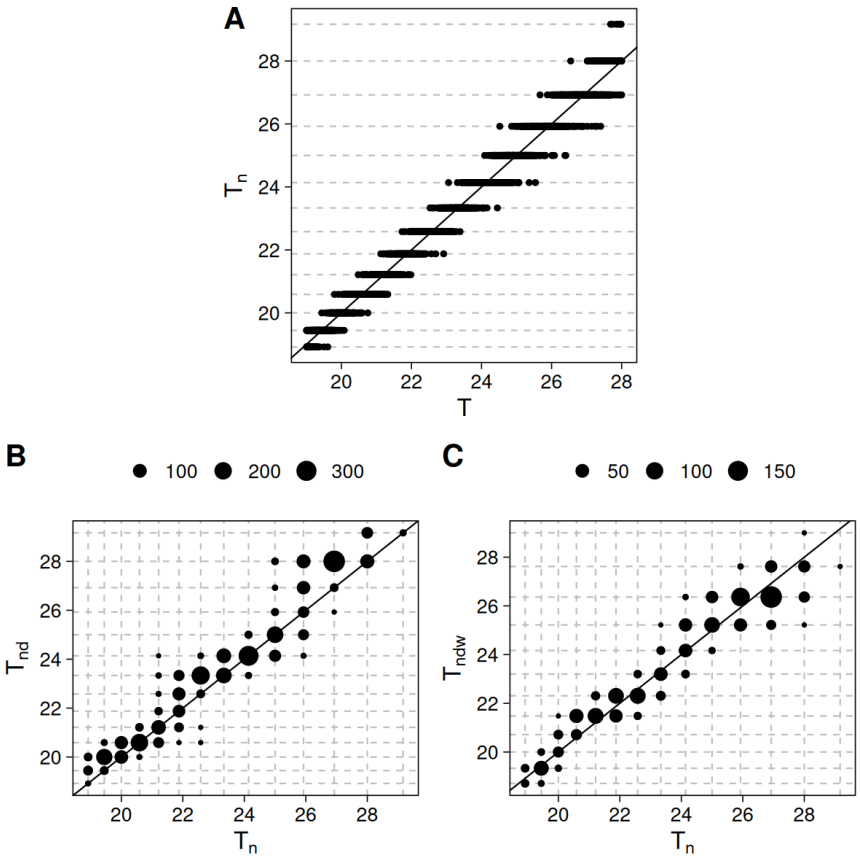

Figure S4: **Accuracy of period determination for different synthetic signals.** **A**: Period T_n estimated for 2000 noisy rhythmic signals generated with T between 19 and 28 hours. **B**: Period T_{nd} estimated for the same signals as in A when decay is applied, as a function of the period estimate T_n of the original signal. **C**: Period T_{ndw} estimated when our method is applied to the signals in B, as a function of the period estimate T_n of the original signal. Horizontal and vertical dashed lines correspond to the values present in the corresponding period grid. In B and C, the size of the symbols is proportional to the number of signals with the periods indicated by the crossing grid lines.

In order to evaluate how good is our method to detect rhythmicity in a signal, independently of the period, we analyzed the p-values obtained for 200 rhythmic and arrhythmic signals. First, Fig. S5 shows that, after decay is added, the p-values of almost all peaks in the periodograms

are above $p = 0.05$, which implies that they would be considered as arrhythmic. When our method is used to eliminate, at least partially, the decaying component, the remaining signals have p-values smaller than 0.05, and would therefore be classified as rhythmic, in 55% of the cases. In other words, there is a 45% of false negatives. This is to be expected since in some cases the combination of noise and decay render almost impossible the recovery of the rhythmic signal. On the other hand, panel B of Fig. S5 shows that, in this case, the method has no false positives, since none of the arrhythmic signal has been classified as rhythmic after detrending is performed.

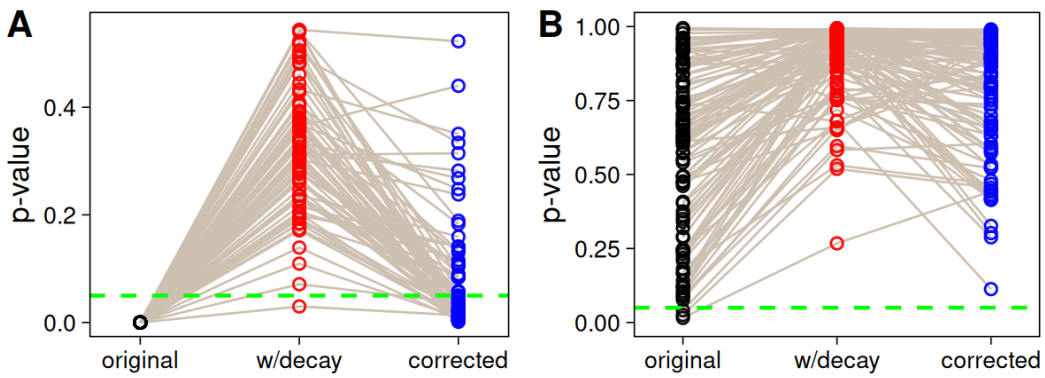

Figure S5: **Presence of false negatives and absence of false positives.** P-values obtained for 100 rhythmic (**A**) and 100 arrhythmic (**B**) synthetic signals. Left: Noisy rhythmic signals. Center: Signals obtained by applying decay to the previous signals. Right: Signals obtained by appplying our method to the previous ones. The green dashed line indicates the level of significance used (0.05).

Example of rhythmicity assessment for a synthetic experiment

As mentioned above, when noise is strong, detrending may not be enough and one must resort to population averaging. To see how well our method performs in this setting, we mimimicked a rhythm assessing experiment on a group of flies by generating 28 rhythmic individual records

of 6 days lengths, using the model described above. The periods T for each record were drawn from a Gaussian with average 23.8 h., and 0.1 h. of statistical deviation. The resulting records are shown in Fig. S6. After the application of our detrending, one can notice that, out of 28 flies, only 5 would be classified as rhythmic (see Fig. S7 for the detrended records and Fig. S8 for the corresponding periodograms). However, when a population average is performed, the resulting periodogram reveals the rhythmicity of the population (Fig. S9).

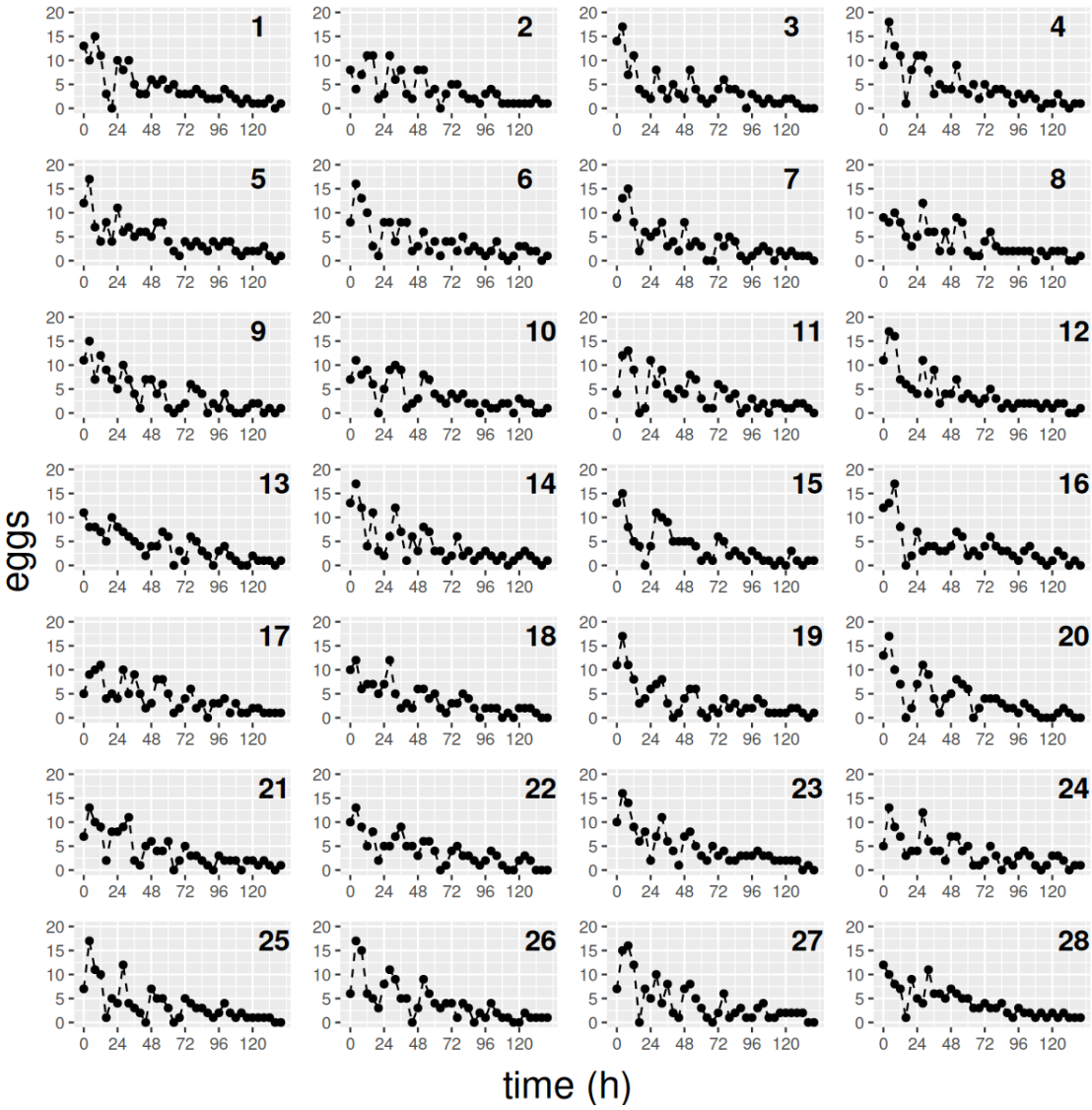

Figure S6: **Individual egg records for the first synthetic experiment with 28 flies.**

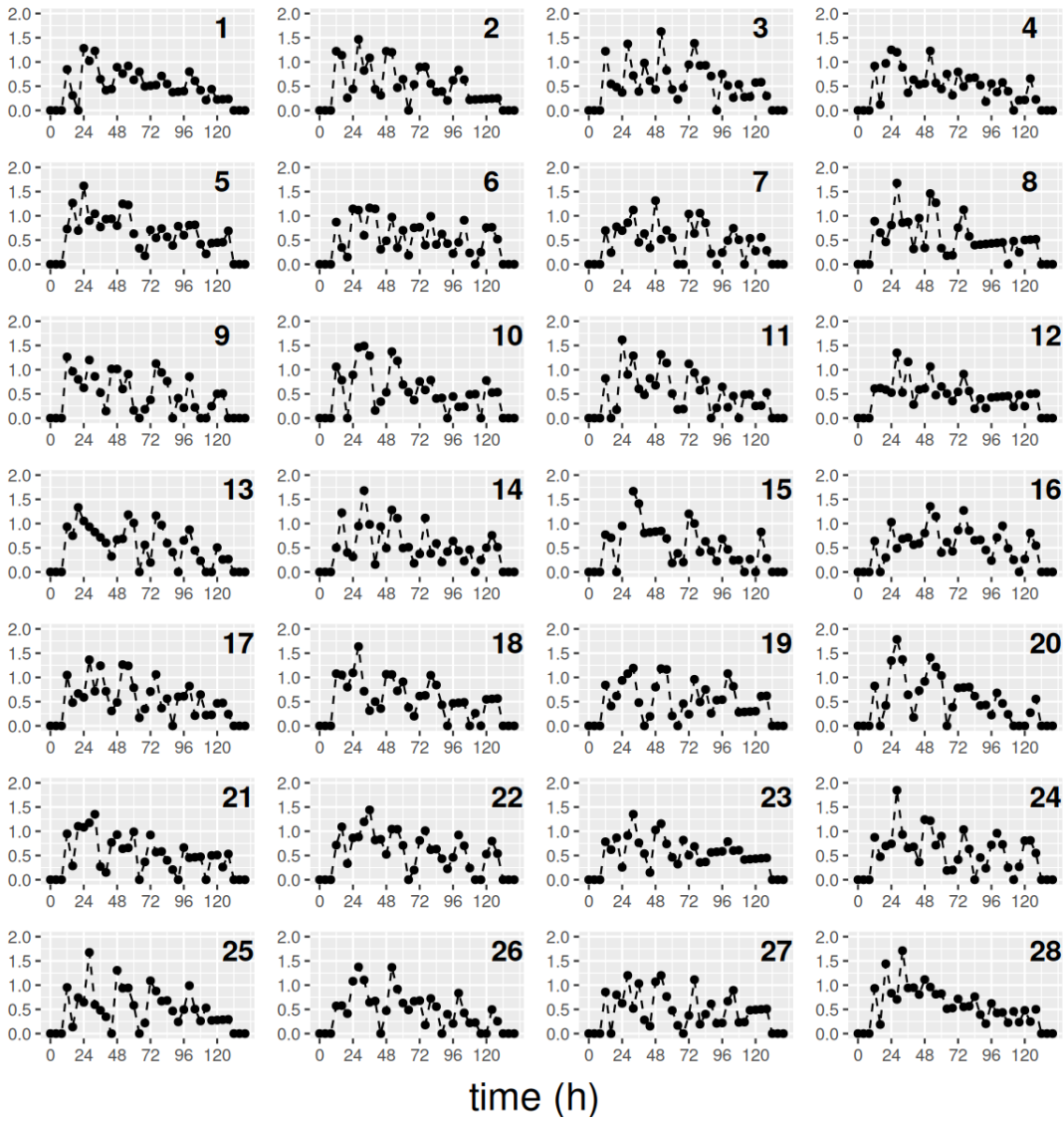

Figure S7: **Records obtained after applying detrending for the first synthetic experiment described in the text.**

As a control, we performed a second synthetic experiment, but now with completely random individual "flies", obtained by using $\alpha = 1$ in Eq. S4. The individual and detrended records, are displayed in Figs. S10, S11, and S12. The population periodogram (Fig. S13A) shows clearly that the population is arrhythmic.

When the population classified as rhythmic, but there are only a few individuals that display

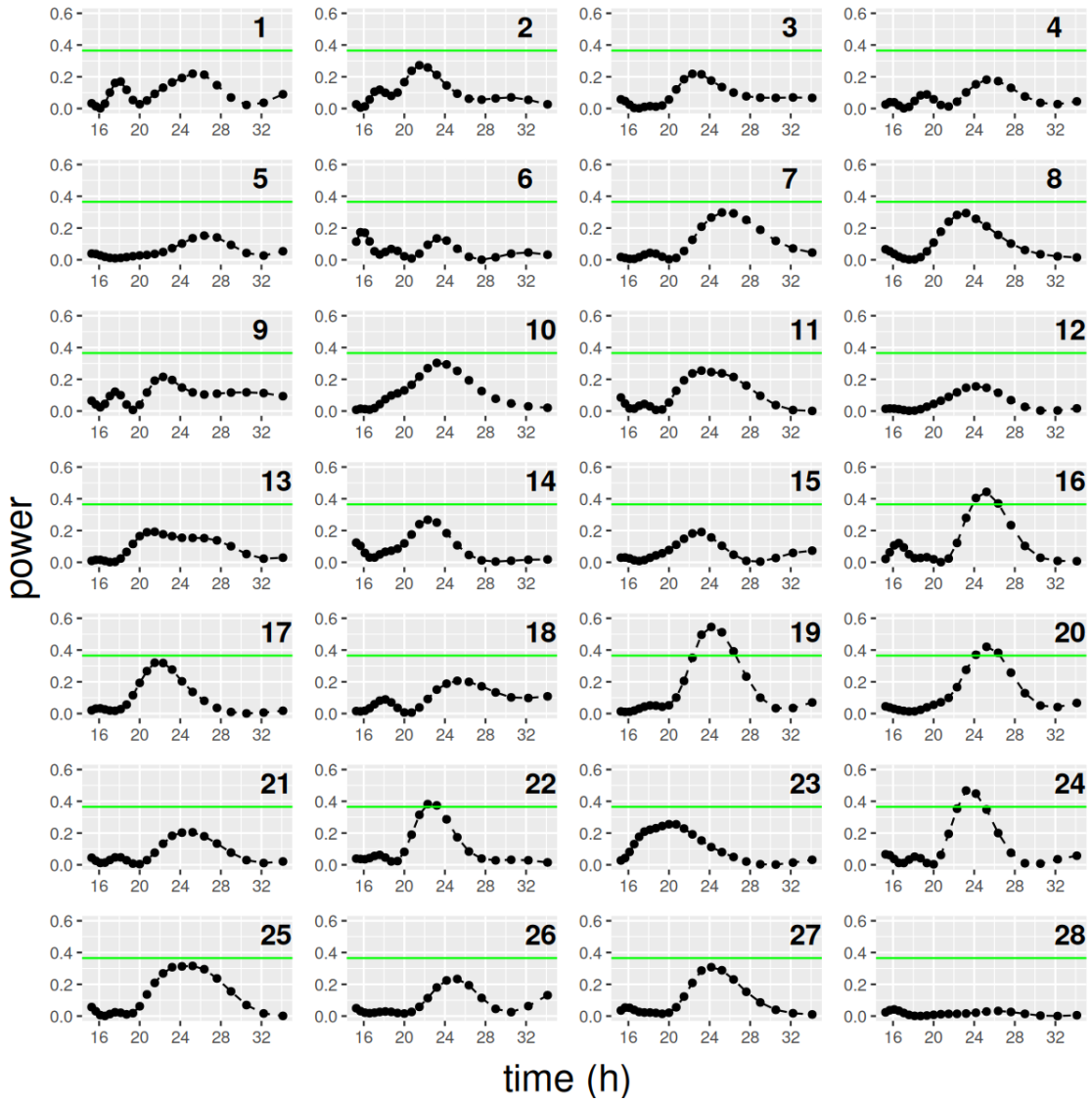

Figure S8: **Periodograms for the records obtained after applying detrending for the first synthetic experiment described in the text.**

a clear rhythmicity, it could be objected that the population rhythm is in fact driven by these very rhythmic individuals. In order to test this possibility, we eliminated the 5 rhythmic records of the first experiment and analyzed the group of the remaining flies. The resulting periodogram is displayed in Fig. S13B. Even though the peak is now lower, the rhythmicity is weaker but still present.

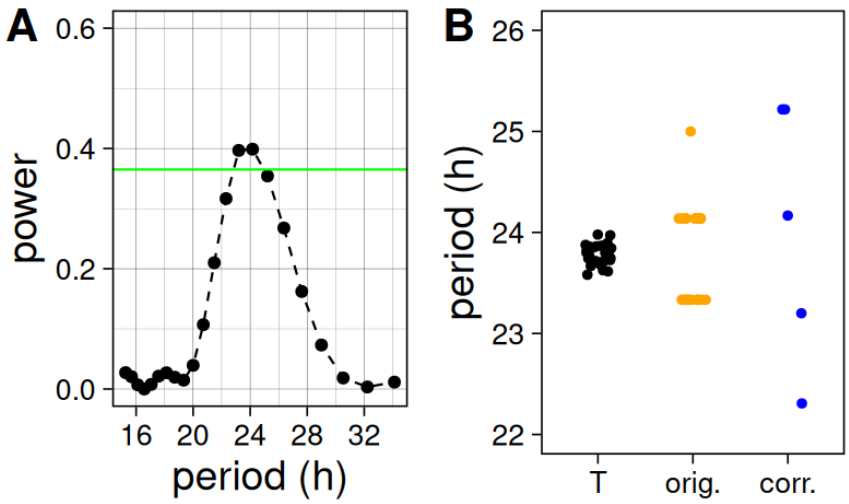

Figure S9: **Results for the first synthetic experiment described in the text.** **A**: Population periodogram. **B**: Individual periods (Left: T of the underlying rhythm, center: period estimate of the signal without decay, right: estimated periods of the records with a significant peak in the periodogram).

Conversely, when 5 random flies of our second experiment (where all flies were truly arrhytmic) are replaced by the 5 rhythmic flies of the first experiment, the population periodogram obtained does not reveal a peak in the population (Fig. S13C).

Example of rhythmicity assessment for a real experiment

In order to check all this in a real experiment, we analyzed the records from two experiments for CantonS and per01 flies. The experiments were performed in DD conditions, using the protocol explained in the main text. The individual records and their corresponding periodograms are shown in Figs. S14 to S19. From Fig. S16 we can check that only 7 flies are individually rhythmic. The population average, however, is strongly rhythmic (see Fig. S20A). We have also assessed the rhythmicity when these individually rhythmic flies are eliminated from the sample. The population average is still rhythmic, albeit with a much reduced power, as was to be expected. It is interesting to compare this with the results obtained for per01 flies, which have been shown

to lack a functional circadian clock. In this case, the average is very arrhythmic, even though one flies appears to be individually rhythmic.

These result confirm that our method can be used to detect rhythms that are usually hidden behind the decay of the signal, and are also strongly contaminated by behavioral noise.

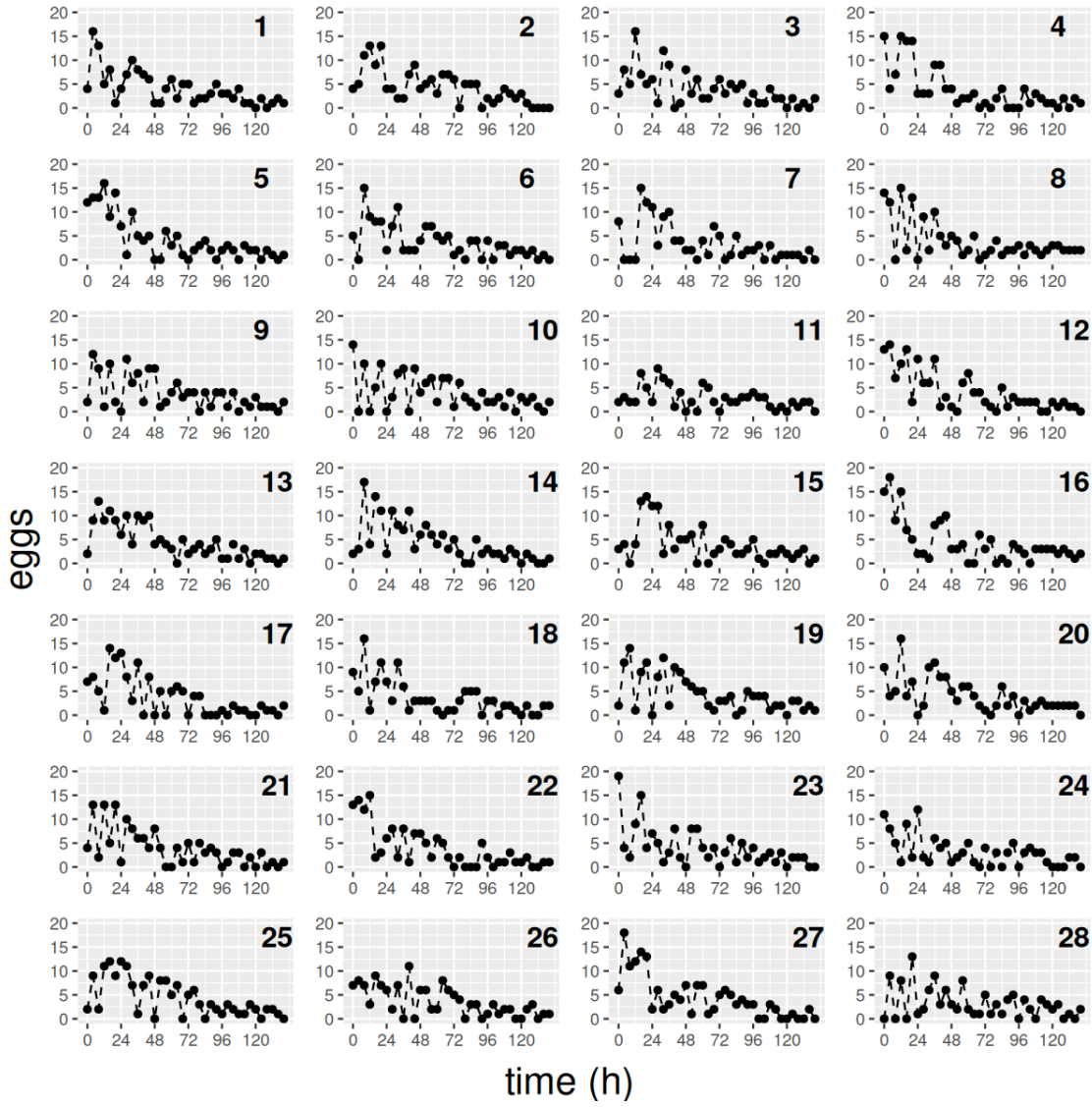

Figure S10: **Individual egg records of the second synthetic experiment with 28 flies.**

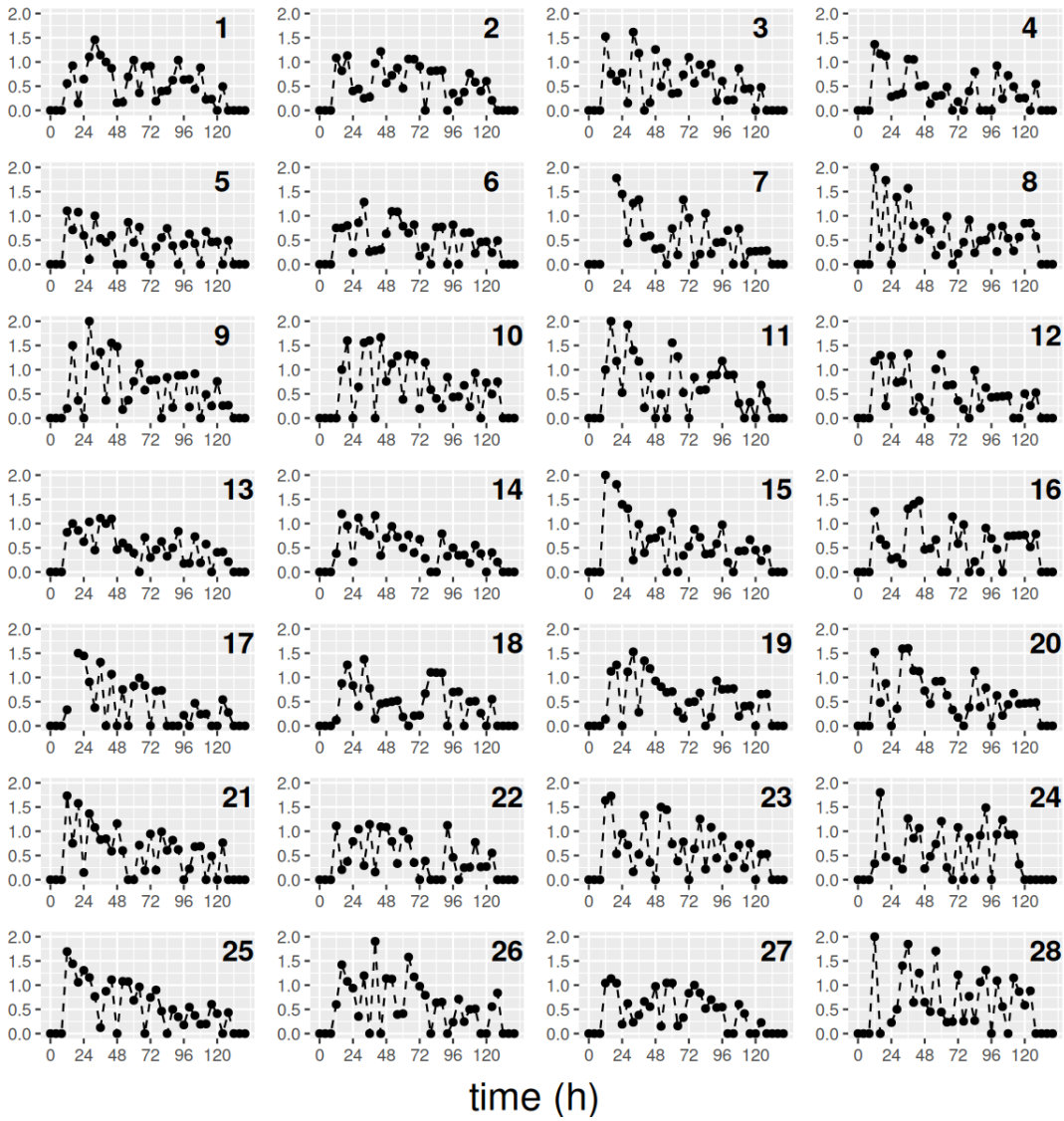

Figure S11: **Records obtained after applying detrending for the second synthetic experiment described in the text.**

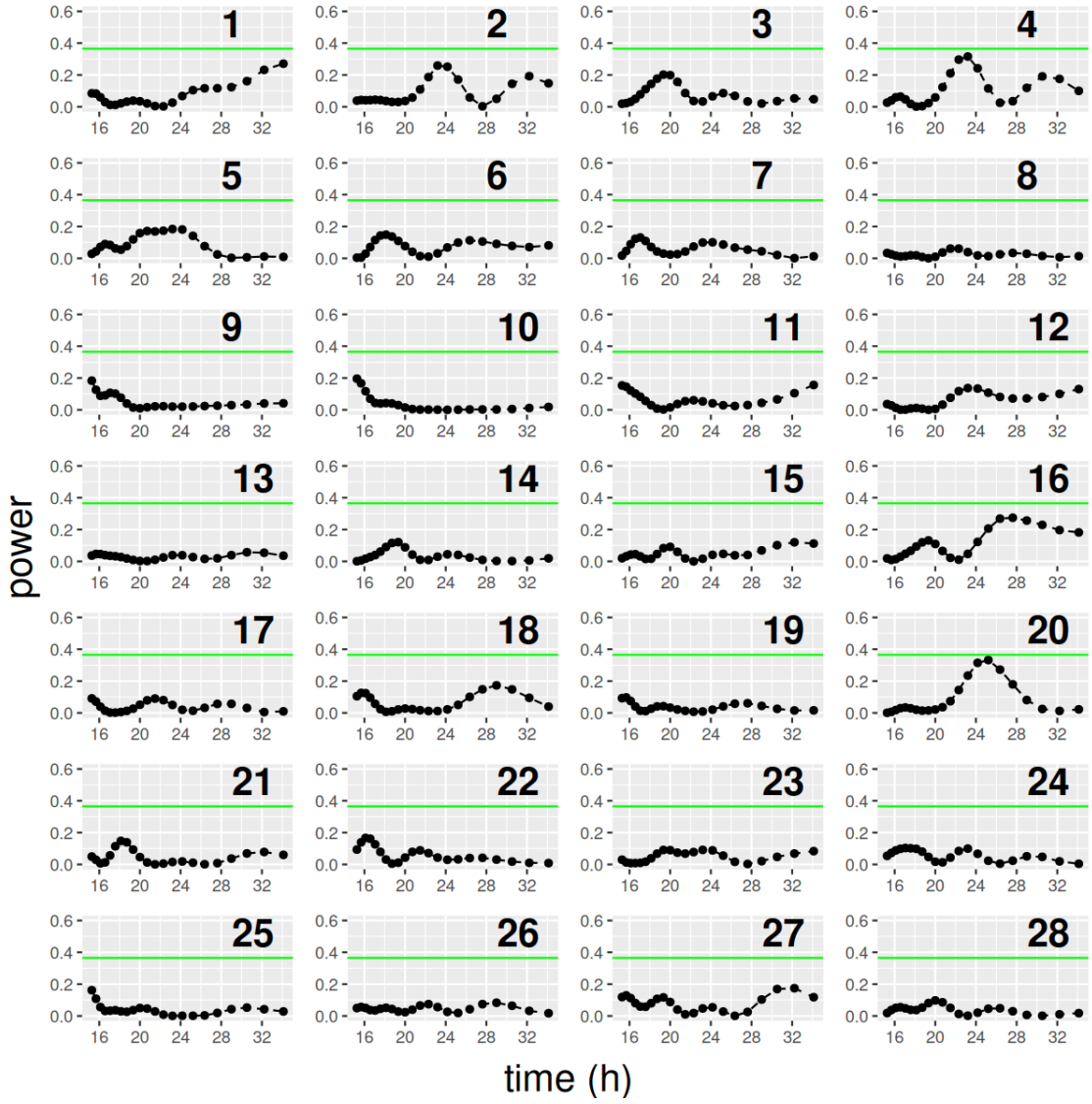

Figure S12: **Periodograms for the records obtained after applying detrending for the second synthetic experiment described in the text.**

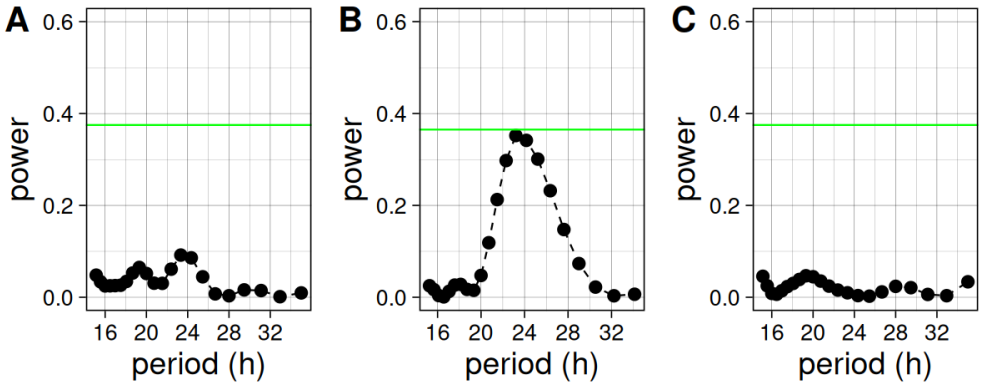

Figure S13: **A few rhythmic flies do not make a population rhythmic.** **A**: Population periodogram for the second experiment mentioned in the text. **B**: Population periodogram for the first experiment without the five most rhythmic flies. **C**: Population periodogram for the second experiment with 5 flies replaced by the 5 rhythmic flies of the first experiment.

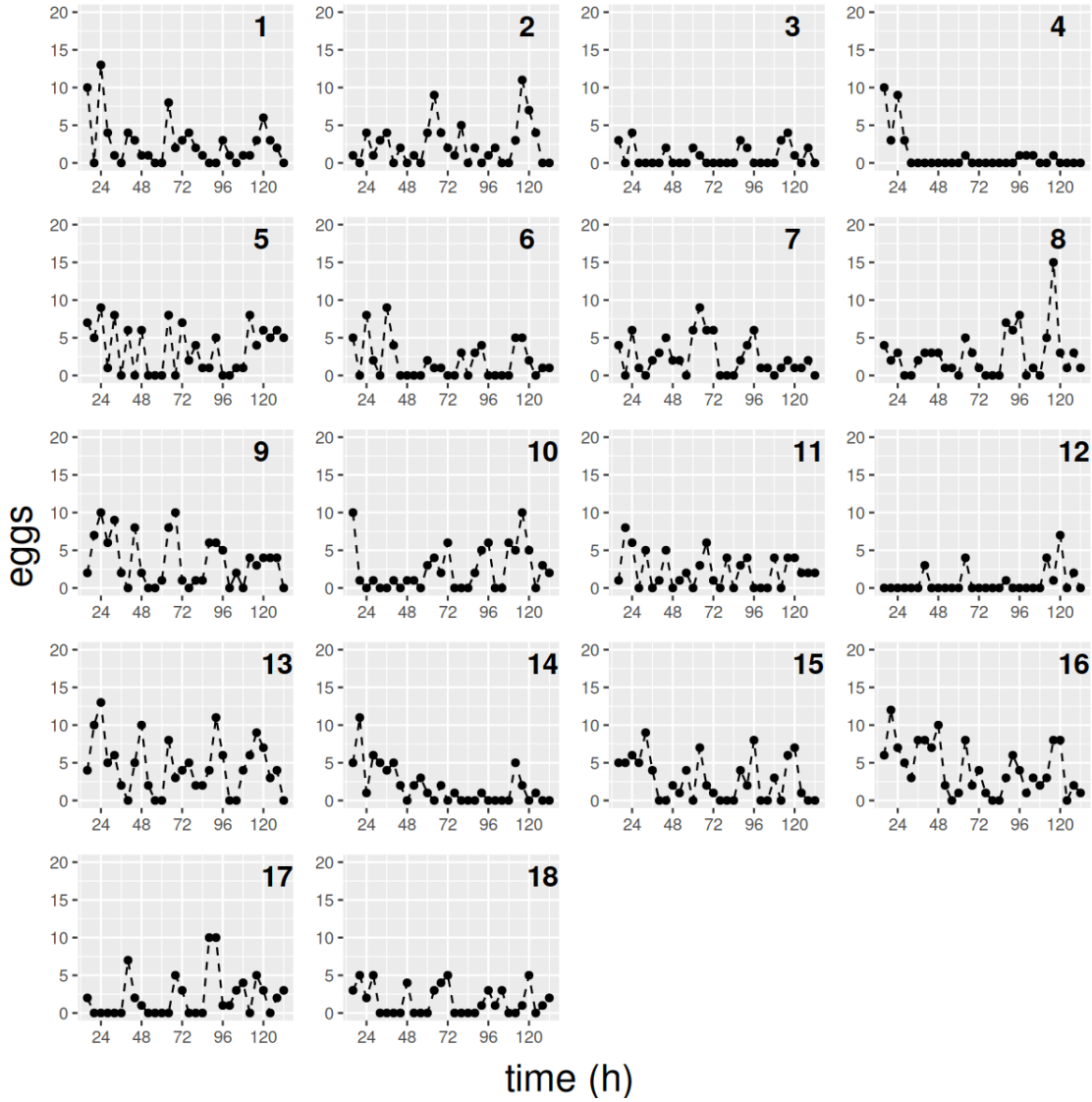

Figure S14: **Individual egg records of an experiment in DD with 18 CantonS female flies.**

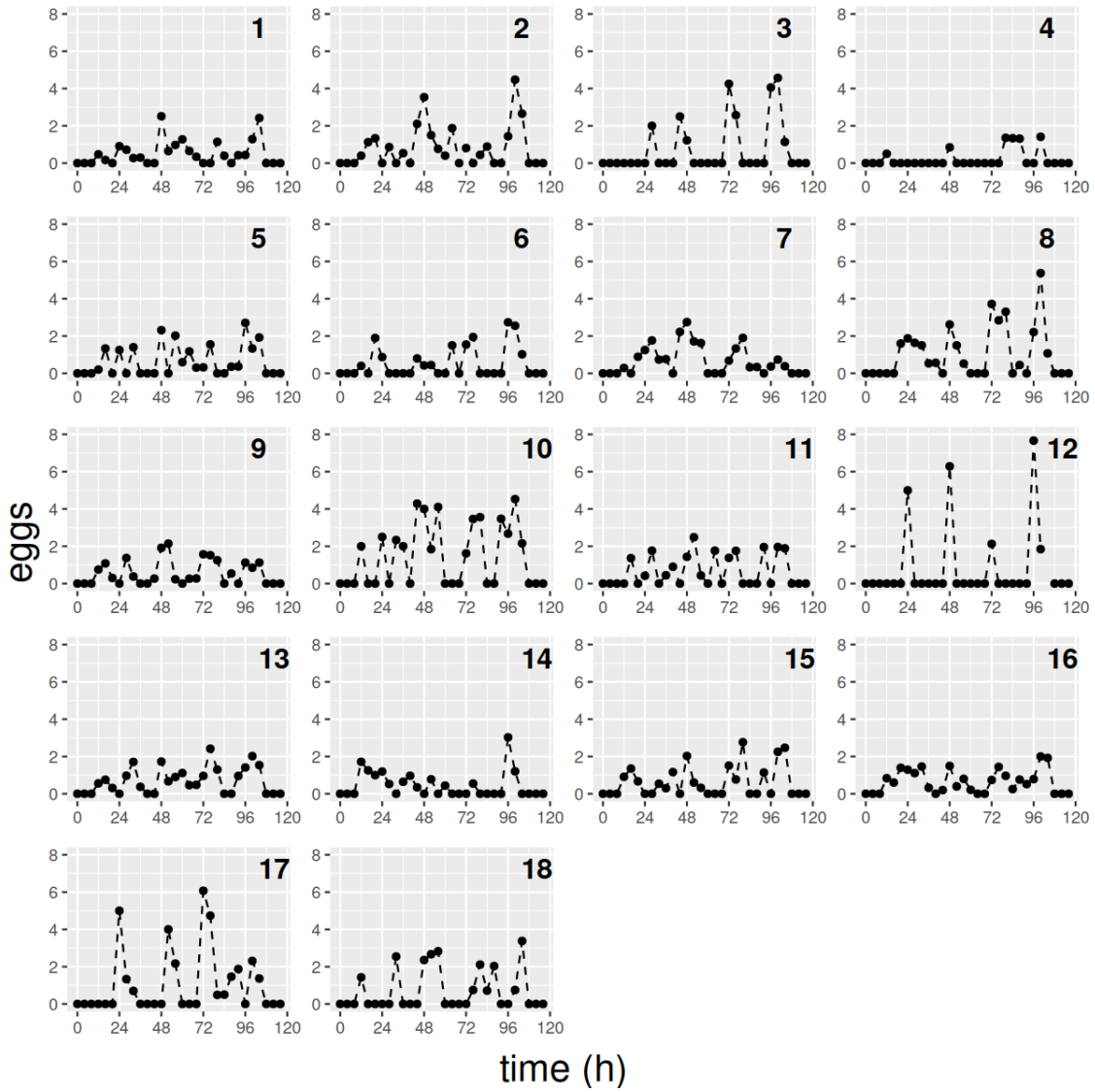

Figure S15: **Records obtained after applying detrending for the experiment in DD with 18 CantonS female flies described in the text.**

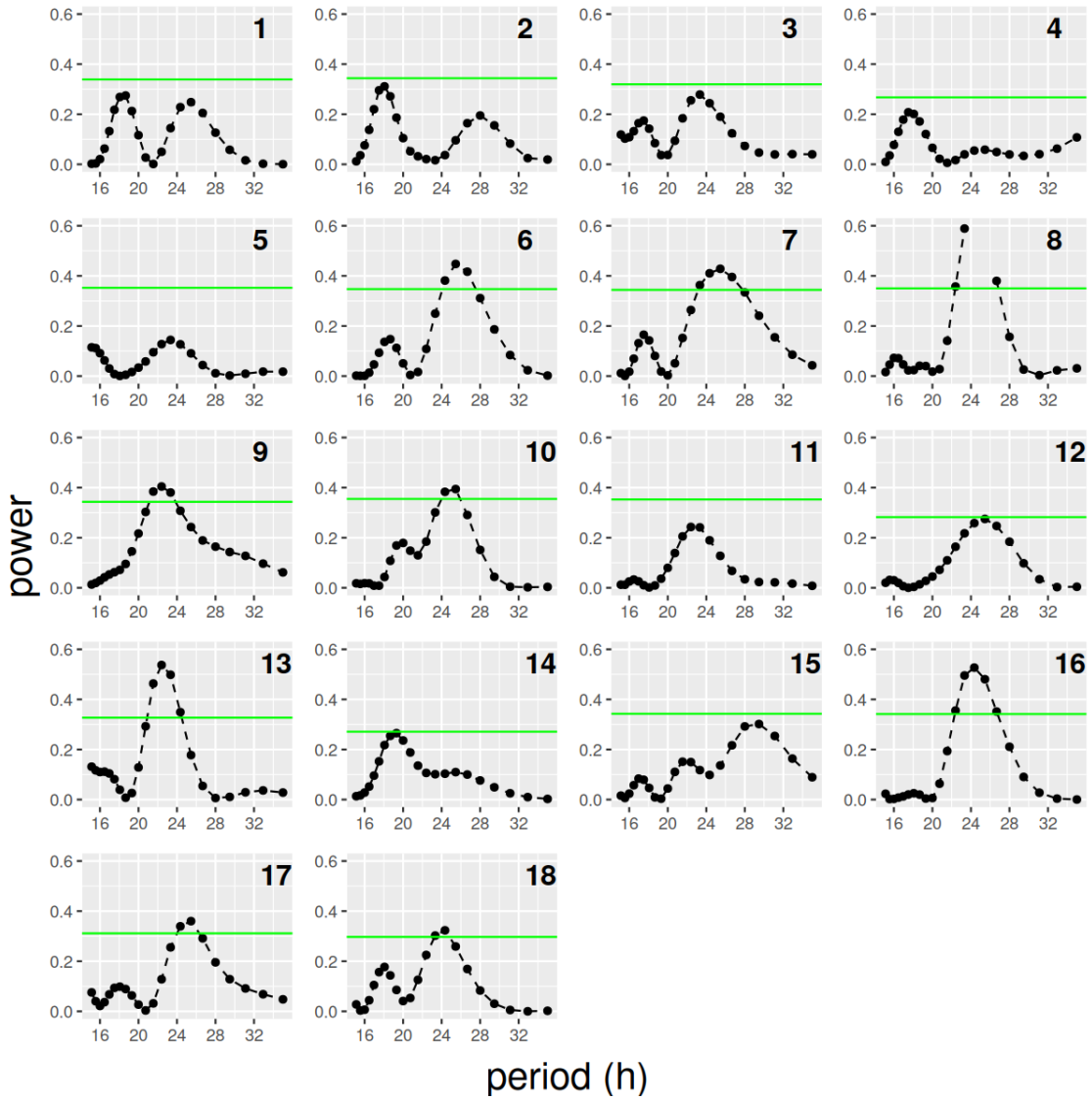

Figure S16: **Periodograms for the records obtained after applying detrending for the experiment in DD with 18 CantonS female flies described in the text.**

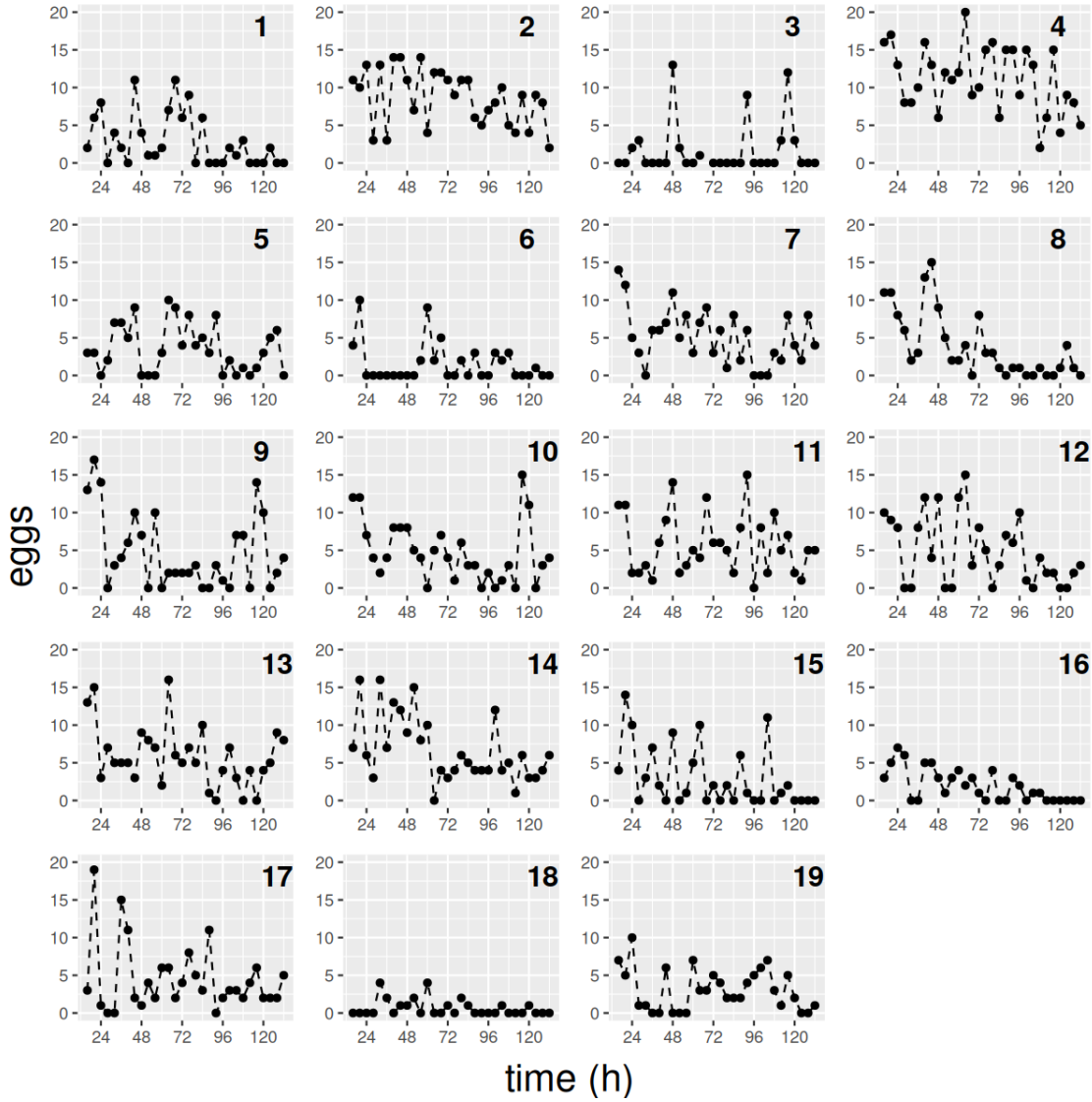

Figure S17: **Individual egg records of an experiment in DD with 19 per01 female flies.**

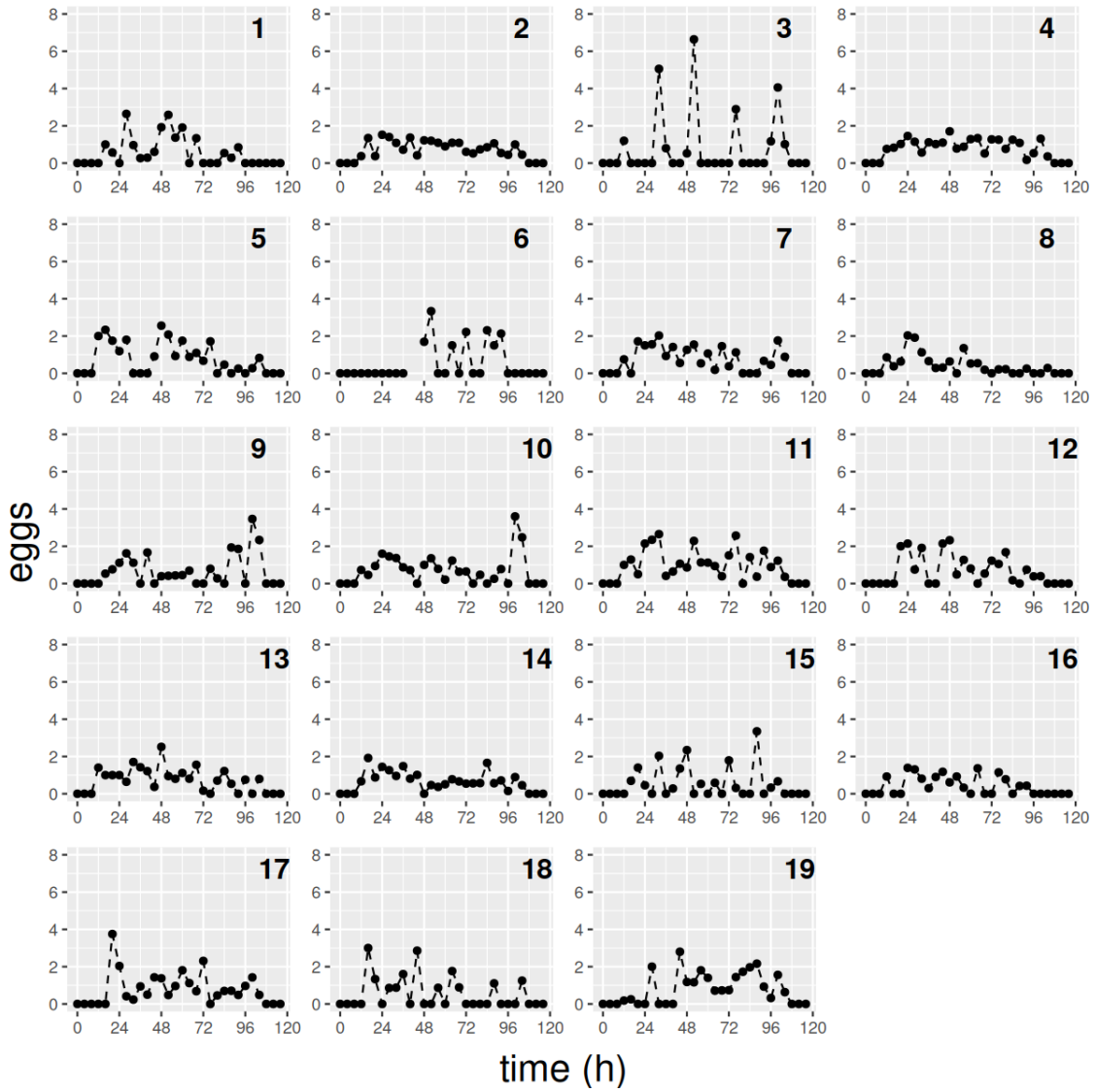

Figure S18: **Records obtained after applying detrending for an experiment in DD with 19 per01 female flies.**

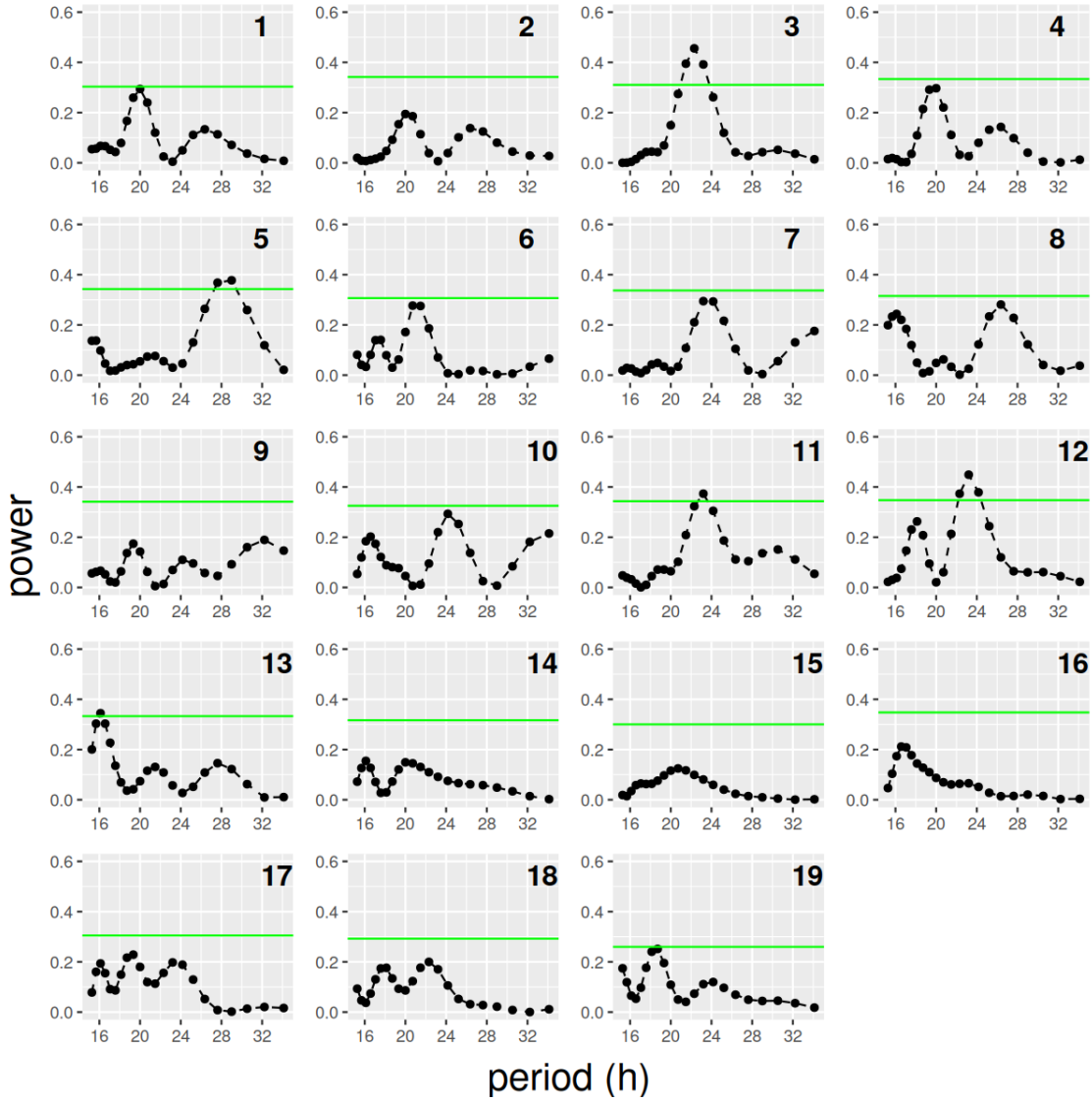

Figure S19: **Periodograms for the records obtained after applying detrending for an experiment in DD with 19 per01 female flies.**

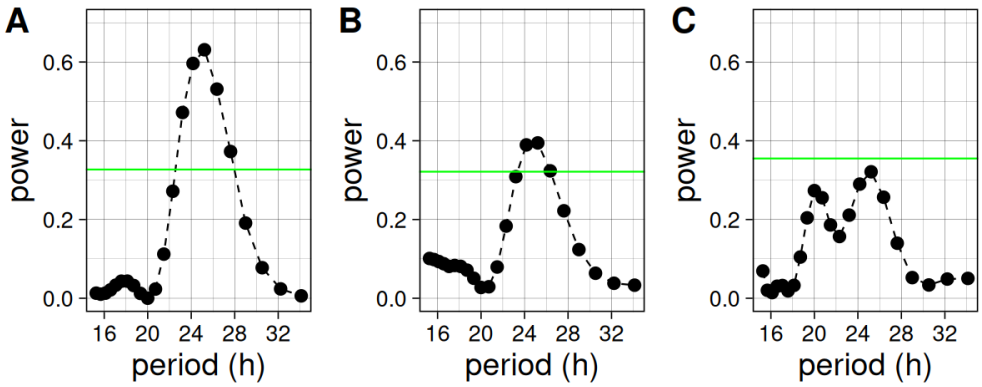

Figure S20: **Persistence of population rhythmicity with or without individually rhythmic flies.** **A**: Population periodogram for the experiment with 18 CantonS female flies mentioned in the text. **B**: Population periodogram for the same experiment as in A, but without 8 individually rhythmic flies. **C**: Population periodogram for the experiment with 19 per01 female flies mentioned in the text

References

Hyndman, R.J. 2021. Forecasting: Principles and Practice (3rd ed.). Otexts.

Semmlow, J. 2018. Signal Analysis in the Time Domain. In Circuits, Signals and Systems for Bioengineers (pp. 51–110). Elsevier.

Ruf, T. 1999. The Lomb-Scargle periodogram in biological rhythm research: Analysis of incomplete and unequally spaced time-series. Biol. Rhythm Res. 30:178–201.

Zielinski T, Moore A. M, Troup E, Halliday K. J, Millar A. J. 2014. Strengths and limitations of period estimation methods for circadian data. PLoS One 9(5):e96462.

Pfeiffenberger C, Lear B. C, Keegan K. P, Allada R. 2010. Processing circadian data collected from the Drosophila Activity Monitoring (DAM) System. Cold Spring Harb Protoc. 2010(11):pdb.prot5519.